Journal of Engineering Mathematics (2024) 145:16
https://doi.org/10.1007/s10665-024-10347-1

An enhanced flux continuity three-dimensional finite element method for heterogeneous and anisotropic diffusion problems on general meshes

Ong Thanh Hai[1,3] · Thi Hoai Thuong Nguyen[1,3] · Anh Ha Le[1,3] · Vuong Nguyen Van Do[2]

Received: 4 August 2023 / Accepted: 19 February 2024 / Published online: 30 March 2024

Abstract
In this research, we present a novel enhanced flux continuity three-dimensional finite element method for heterogeneous and anisotropic (possibly discontinuous) diffusion problems on general meshes. We create a polygonal dual mesh $\mathcal{T}_h^*$ and its submesh $\mathcal{T}_h^{**}$ from a primal mesh $\mathcal{T}_h$ in such a manner that a set number of adjacent tetrahedral elements of $\mathcal{T}_h^{**}$ are united to form each dual control volume of $\mathcal{T}_h^*$, which corresponds to a primal vertex. The weak solution of the diffusion problem is approximated by the piecewise linear functions on the subdual mesh $\mathcal{T}_h^{**}$. In order to capture the local continuity of numerical fluxes across the interfaces, the proposed scheme gives the auxiliary face unknowns interpolated by the multi-point flux approximation. Moreover, the consistency, coercive, and convergence properties of the method are presented within a rigorous theoretical framework. Numerical results are carried out to highlight accuracy and efficiency.

Keywords Finite element · General meshes · Heterogeneous anisotropic (possibly discontinuous) diffusion · Numerical flux continuity

✉ Ong Thanh Hai
othai@hcmus.edu.vn

Thi Hoai Thuong Nguyen
ngththuong@hcmus.edu.vn

Anh Ha Le
laha@hcmus.edu.vn

Vuong Nguyen Van Do
donguyenvanvuong@tdtu.edu.vn

1 Department of Analysis, Faculty of Mathematics & Computer Science, University of Science, 227 Nguyen Van Cu, Ho Chi Minh 700000, Vietnam

2 Applied Computational Civil and Structural Engineering Research Group, Faculty of Civil Engineering, Ton Duc Thang University, Ho Chi Minh, Vietnam

3 Vietnam National University, Ho Chi Minh 700000, Vietnam

Mathematics Subject Classification 65N30 · 65N08 · 76S05

1 Introduction

The three-dimensional heterogeneous and anisotropic diffusion problems arising in the wide range of fields have considerably drawn much attention from researchers in many scientific applications such as oil reservoir simulation, hydrogeology, semiconductor, biology model, and plasma physics. Particularly, we consider the following problem on an open bounded connected polyhedral domain Ω in $\mathbb{R}^3$:

$$-\operatorname{div}(\Lambda \nabla u) = f \quad \text{in } \Omega, \tag{1}$$

with the homogeneous Dirichlet boundary condition:

$$u = 0 \quad \text{on } \partial\Omega. \tag{2}$$

The source term f belongs to $L^2(\Omega)$. The tensor Λ is piecewise Lipschitz continuous on Ω, and satisfied symmetric, positive definite. Therefore, for almost every $x \in \Omega$, we have

$$\underline{\lambda}|\boldsymbol{\xi}|^2 \leq \Lambda(x)\boldsymbol{\xi} \cdot \boldsymbol{\xi} \leq \overline{\lambda}|\boldsymbol{\xi}|^2, \quad \forall \boldsymbol{\xi} \in \mathbb{R}^3, \tag{3}$$

where $\underline{\lambda}$ and $\overline{\lambda}$ are positive values.

The variational form of (1) can be represented as

$$\begin{aligned} &\text{Find } \overline{u} \in \mathcal{H}_0 := H_0^1(\Omega) \text{ such that} \\ &\int_\Omega \Lambda(x)\nabla\overline{u}(x) \cdot \nabla v(x)dx = \int_\Omega f(x)v(x)dx, \quad \forall v \in H_0^1(\Omega). \end{aligned} \tag{4}$$

For this problem, we developed a novel efficient method to accurately approximate the weak solution $\overline{u}$. When carrying out this work, we met the following two main difficulties: (i) the continuity of numerical fluxes regarding to the heterogeneous and anisotropic diffusion problems (possibly discontinuous) must be imposed on the numerical methods; (ii) they are designed to handle on general meshes. Note that the standard finite element method cannot pass two challenges (i) and (ii).

In the literature of numerical methods for the problem (1)–(2), the finite volume method is well known to find the approximate solutions of the heterogeneous and anisotropic problems (4) on admissible meshes. The two-point formula, which is used in this method to approximate the diffusion flux $-\int_{\mathfrak{f}} \Lambda(x)\nabla\overline{u}(x) \cdot \mathbf{n}_{K,\sigma}dx$ through any face f of each control volume K, guarantees the local conservation of the discrete fluxes. Note that the geometry of grid cells is admissible to ensure the consistency property of the two-point flux approximation. In [1], the authors proposed a cell-centered finite volume scheme which treats material discontinuities for three-dimensional diffusion equation. Its discrete normal flux is approximated by a linear combination of

the directional flux along the line connecting cell centers and the tangent flux along the cell faces. However, the problem is only considered on a scalar diffusion coefficient.

Along with the cell-centered techniques, the potent hybrid techniques have been successfully used to polygonal and polyhedral meshes, both structured and unstructured, that include extra unknowns on the edges, faces, and vertices in order to approximate the solution $\overline{u}$. In particular, we first mention the mixed finite element method having the Raviart–Thomas basis functions. Its unknowns are the discrete fluxes and discrete gradients. This method demands high refined grids to apply for some highly heterogeneous and anisotropic cases. In [2], the authors introduced the mixed finite volume method (MFV) based on the original developments from the finite volume. This method can be carried out for any mesh type in arbitrary space dimension, and possesses the fluxes and the cell-centered unknowns. We also have the hybrid finite volume (HFV) methods [3] using both cell and edge unknowns. Giving another approach, the extensions of the discrete duality finite volumes (DDFV) method for applications to three-dimensional diffusion problems are the CeVeFE-DDFV [4], the CeVeDDFV-A [5], and the CeVeDDFV-B [6] methods. These methods are shown to be complicated when applied to solving many engineering problems with diffusion terms on a complex geometric computed domain. This is because the discrete gradient, the discrete divergence, the discrete duality property, and the kernel of the discrete gradient can be difficult to compute (e.g., volumes, faces) and describe for more complex geometries of the boundary faces, the primal, secondary, diamond cells (see [7, Remark 6], [6, Eq. (2)]). In addition, these schemes are limited to polyhedral cells whose faces have only three or four sides. According to the literature review, the numerical methods still have some mentioned drawbacks when applying to the three-dimensional heterogeneous and anisotropic diffusion problems. From the above drawbacks of the current schemes, our objective for this work is to investigate a novel enhanced flux continuity three-dimensional finite element method (EFC-3DFEM) for heterogeneous and anisotropic diffusion problems (4) on the general meshes. The EFC-3DFEM scheme includes the following advantages:

1. Given a general primal mesh, the method is suitable for constructing the dual and tetrahedral subdual meshes, ensuring that each dual control volume is indeed a macroelement, the union of a fixed number of adjacent tetrahedra from the subdual mesh $\mathcal{T}_h^{**}$ (see [8, pp. 497–498]). The approximate space for the solution $\overline{u}$ of (4) has piecewise linear basis functions on the tetrahedral subdual mesh $\mathcal{T}_h^{**}$;
2. In order to guarantee the local continuity of fluxes, the discrete gradient and fluxes are taken into account the anisotropic, heterogeneous tensor Λ (potentially discontinuous) using the multi-point flux approximation approach;
3. With a mild assumption on geometry, the linear system is always symmetric and positive definite, this helps to reduce the computational cost by the iterative methods for solving linear systems;
4. The scheme provides the exact solution u of (1), if the tensor Λ is piecewise constant in polygonal sub-domains and the exact solution u is affine in each of these sub-domains;
5. The scheme is demonstrated to achieve both strong dual consistencies and coercive properties. Consequently, the approximate solution converges to the weak solution

$\overline{u}$ as the mesh size tends to 0, even for fully heterogeneous anisotropic (possibly discontinuous) diffusion problems;
6. The tetrahedral subdual mesh $\mathcal{T}_h^{**}$ is built as an improved primal mesh, which allows the scheme to provide greater precision at a same computational cost; and
7. Since the standard finite element programs which are based on tetrahedral meshes, thus they may be used directly, the algorithm is simple to implement.

The framework of this study is organized as follows: in Sect. 2, we describe in detail the construction of the dual mesh $\mathcal{T}_h^*$ and its subdual meshes $\mathcal{T}_h^{**}$. Section 3 presents the discretization of the EFC-3DFEM scheme to obtain a well-posed discrete variational problem. It evidences that the associated linear algebraic system is positive definite and symmetric, then it has the unique solution. In Sect. 4, the scheme is verified for strong, dual consistencies and coercive properties. With these properties, we can present the proof of the convergent results based on [3, Lemma 2.2]. Section 5 compares the results of numerical experiments [9] for the diffusion issue with the heterogeneous and anisotropic tensor (potentially discontinuous) and various mesh types. The paper is concluded in the last section.

2 Construction of meshes

In this part, we go through how to create a dual mesh from a given primal mesh, along with its submesh.

2.1 The primal mesh

Consider a discretization of Ω defined as a collection $\mathcal{D} = (\mathcal{T}_h, \mathcal{V}, \mathcal{C}, \mathcal{E}, \mathcal{F})$ with

a. $\mathcal{T}_h$ is a subset of Ω that is a family of non-empty, open, connected disjoint subsets such that

$$\bigcup_{K \in \mathcal{T}_h} \overline{K} = \overline{\Omega}.$$

For each $K \in \mathcal{T}_h$, we denote its volume by m_K, its circumscribed sphere's diameter by h_K, and let $h = \max\{h_K,\ \forall K \in \mathcal{T}_h\}$.
b. $\mathcal{V}$ is a set of all vertices of $\mathcal{T}_h$. We denote two sets of all vertices inside Ω, and of all vertices on $\partial\Omega$ by $\mathcal{V}_\Omega$ and $\mathcal{V}_{\partial\Omega}$, respectively.
c. $\mathcal{C}$ is a set of all mesh points of $\mathcal{T}_h$. Its elements are defined as follows: for each $K \in \mathcal{T}_h$, its associated mesh point x_K is an interior point in K such that the segment $[x_K, x]$ lies inside K for all points $x \in K$.
d. $\mathcal{E}$ is a set of all edges of $\mathcal{T}_h$. Its two subsets $\mathcal{E}_\Omega$ and $\mathcal{E}_{\partial\Omega}$ contain interior edges and boundary edges, respectively. For each edge $\mathtt{e} \in \mathcal{E}$, we denote the midpoint of $\mathtt{e}$ by $x_\mathtt{e}$ which is collected in the set $\mathcal{C}_\mathcal{E}$, and has two subsets $\mathcal{C}_{\mathcal{E}_\Omega} = \{x_\mathtt{e} \mid e \in \mathcal{E}_\Omega\}$ and $\mathcal{C}_{\mathcal{E}_{\partial\Omega}} = \{x_\mathtt{e} \mid e \in \mathcal{E}_{\partial\Omega}\}$.
e. $\mathcal{F}$ is a set of all faces of $\mathcal{T}_h$ whose two subsets consist of $\mathcal{F}_\Omega = \{\mathtt{f} \mid \mathtt{f} \text{ inside } \Omega\}$ and $\mathcal{F}_{\partial\Omega} = \{\mathtt{f} \mid \mathtt{f} \text{ on } \partial\Omega\}$. For each $\mathtt{f} \in \mathcal{F}_\Omega$, there exist exactly two primal control

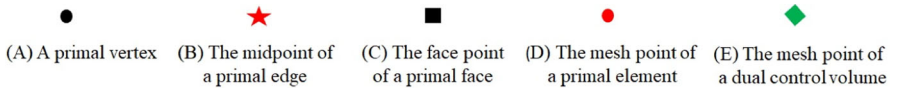

Fig. 1 A primal vertex, the midpoint of a primal edge, the face point of a primal face, and the mesh point of a primal element are represented by the symbols in (A), (B), (C), and (D)

volumes $K, L \in \mathcal{T}_h$ sharing the common face $\mathtt{f}$. Supposed that a segment joining two points x_K and x_L intersects with $\mathtt{f}$ at a point $x_\mathtt{f}$ called the face point of $\mathtt{f}$. For each $\mathtt{f} \in \mathcal{F}_{\partial\Omega}$, a face point $x_\mathtt{f}$ is an inner point of $\mathtt{f}$ such that for any $x \in \mathtt{f}$, $[x_\mathtt{f}, x] \in \mathtt{f}$. These face points are collected in the set $\mathcal{C}_\mathcal{F} = \mathcal{C}_{\mathcal{F}_\Omega} \cup \mathcal{C}_{\mathcal{F}_{\partial\Omega}}$, where $\mathcal{C}_{\mathcal{F}_\Omega} = \{x_\mathtt{f} \mid \mathtt{f} \in \mathcal{F}_\Omega\}$ and $\mathcal{C}_{\mathcal{F}_{\partial\Omega}} = \{x_\mathtt{f} \mid \mathtt{f} \in \mathcal{F}_{\partial\Omega}\}$.

For the sake of simplicity, Fig. 1 introduces some symbols to points of these above sets.

2.2 The dual mesh

The dual mesh is described as a collection $\mathcal{D}^* = \left(\mathcal{T}_h^*, \mathcal{V}^*, \mathcal{C}^*, \mathcal{E}^*, \mathcal{F}^*\right)$ with $\mathcal{T}_h^*$, $\mathcal{V}^*$, $\mathcal{C}^*$, $\mathcal{E}^*$, and $\mathcal{F}^*$ are the sets of the dual control volumes, dual vertices, dual mesh points, dual edges, and triangular dual faces, respectively. The dual mesh is later utilized to construct the tetrahedral submesh. To create the dual mesh $\mathcal{D}^*$ (see Algorithm 1), we apply the method described in [10, Section 2] (with minor adjustments).

Algorithm 1 The construction of the dual mesh

Step 1: Establish a dual vertex for each mesh point x_K of the primal element K in $\mathcal{T}_h$.
Step 2: Establish a dual vertex at the face point $x_\mathtt{f}$ of each primal boundary face $\mathtt{f}$ in $\mathcal{F} \cap \partial\Omega$.
Step 3: Establish a dual vertex at the midpoint $x_\mathtt{e}$ of each primal edge $\mathtt{e}$ in $\mathcal{E}$.
Step 4: Establish a dual vertex at each primal boundary vertex x_V in $\mathcal{V} \cap \partial\Omega$.

Step 5: Establish triangular dual faces that match to the primal edges.
Step 6: Establish triangular dual faces that match to the primal boundary vertices.

Step 7: Establish dual control volumes that correspond to primal vertices.
Step 8: Establish mesh points for dual control volumes.

Next, we describe in detail the implementation of each step in Algorithm 1 as follows:

Constructing dual vertices

Step 1: The corresponding dual vertex of each primal element K in $\mathcal{T}_h$ is selected to represent the mesh point x_K of K.

Step 2: Additionally, there are dual vertices at the face point $x_\mathtt{f}$ of each primal boundary face $\mathtt{f}$ in $\mathcal{F} \cap \partial\Omega$.

Step 3: The midpoint $x_\mathtt{e}$ of each primal edge $\mathtt{e}$ in $\mathcal{E}$.

Step 4: The primal boundary vertices x_V in $\mathcal{V} \cap \partial\Omega$.

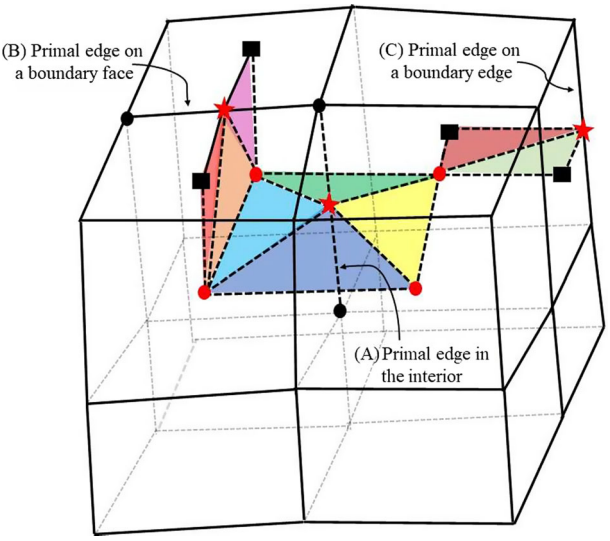

Fig. 2 Triangular dual faces correspond to multiple primordial edges that are either in the domain interior (A, four triangles), on a boundary edge (B, three triangles), or on a boundary edge (C, two triangles)

Constructing dual faces

Dual faces are formed by both primal edges and primal boundary vertices. We note that in our architecture, the "face" are often not $\mathbb{R}^3$ hyperplanes, but rather $\mathbb{R}^2$ surfaces combinations. We generate the corresponding triangular dual faces (Step 5) for each primal edge $\mathtt{e}$ in $\mathcal{E}$ as follows:

Step 5 (a): If $\mathtt{e}$ is inside of Ω, we can begin to construct a "face" by progressively traversing all of its related primordial elements in a single direction. We get triangular dual faces by utilizing this "face" and attaching the midpoint $x_{\mathtt{e}}$ (of $\mathtt{e}$) to all of the vertices (see label A in Fig. 2).

Step 5 (b): There are two primordial boundary faces, $\mathtt{f}^1_{\partial\Omega,\mathtt{e}}$ and $\mathtt{f}^2_{\partial\Omega,\mathtt{e}}$ that share the edge $\mathtt{e}$ if $\mathtt{e}$ is on the boundary $\partial\Omega$. This allows us to also generate a "face" in this case. The algorithm begins at one of the two primal boundary faces, say $\mathtt{f}^1_{\partial\Omega,\mathtt{e}}$, and proceeds through the set $\mathcal{T}_{\mathtt{e}}$ of all primal elements with $\mathtt{e}$ as their edges until it reaches the other boundary face $\mathtt{f}^2_{\partial\Omega,\mathtt{e}}$, and then connects the midpoint of $\mathtt{e}$ with the mesh point of $\mathtt{f}^1_{\partial\Omega,\mathtt{e}}$, the dual vertices x_K, for all K in $\mathcal{T}_{\mathtt{e}}$ and the mesh point of $\mathtt{f}^2_{\partial\Omega,\mathtt{e}}$.
Finally, the "face" is created by connecting the last mesh point of $\mathtt{f}^2_{\partial\Omega,\mathtt{e}}$ to the midpoint of $\mathtt{e}$. The triangular dual faces are then formed by connecting the midpoint $x_{\mathtt{e}}$ of $\mathtt{e}$ to all vertices of this "face" (see labels B and C in Fig 2).

Step 6 (a): For each primal boundary vertex x_V in $\mathcal{V} \cap \partial\Omega$, we designate $\mathcal{F}_{x_V}$ as a set of primal boundary faces, and $\mathcal{E}_{x_V}$ as a set of edges with x_V as their vertex,

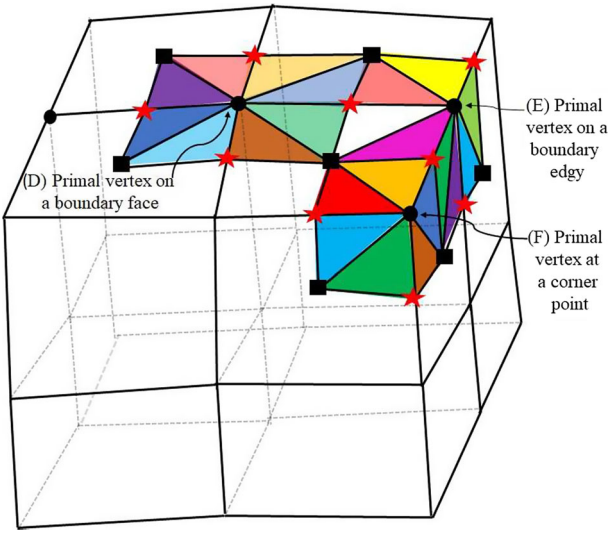

Fig. 3 Triangular dual faces (used for boundary capping) correspond to a number of primordial boundary vertices, including those on a boundary face (D), a 2-manifold boundary edge (E), and a corner point (F)

in the same way. There are two edges $\mathfrak{e}_{\mathfrak{f},1}, \mathfrak{e}_{\mathfrak{f},2}$ in $\mathcal{E}_{x_V}$ that correspond to the boundary $\partial\mathfrak{f}$ for each $\mathfrak{f}$ in $\mathcal{F}_{x_V}$. The procedure for constructing the "face" corresponding to x_V begins at the midpoint $x_{\mathfrak{e}_{\mathfrak{f},1}}$ for some $\mathfrak{f} \in \mathcal{F}_{x_V}$ and connects to the face point $x_{\mathfrak{f}}$ and the midpoint $x_{\mathfrak{e}_{\mathfrak{f},2}}$; continue until returning to the original point which is the midpoint $x_{\mathfrak{e}_{\mathfrak{f},1}}$.

Step 6 (b): By using this "face," we connect the boundary vertex x_V with all of its vertices to create triangular dual faces.

Obviously, the triangular dual face construction can be generated with the boundary $\partial\Omega$ by taking the intersection of multiple faces (see labels D, E, and F in Fig. 3). The aforementioned steps are designed to produce capping "face" that match to boundary primordial vertices, guaranteeing that the boundary $\partial\Omega$ is represented with the same accuracy in both the dual mesh and the primary mesh.

Creating dual control volumes corresponding to primal vertices

Polyhedrons M of the dual mesh $\mathcal{T}_h^*$ are constructed by gathering all the triangular dual faces corresponding to one primal vertex $x_V \in \mathcal{V}$ (Step 7). There are two cases:

Step 7 (a): If x_V is in the interior of Ω, then its related dual control volume M_{x_V} is formed from all triangular dual faces associated with primal edges connected to x_V (see label A in Fig. 4).

Step 7 (b): If x_V is on the boundary $\partial\Omega$, M_{x_V} is formed from the triangular dual faces of primal edges connected to x_V and covered with the boundary triangular dual faces corresponding to x_V (see labels B and C in Fig. 4).

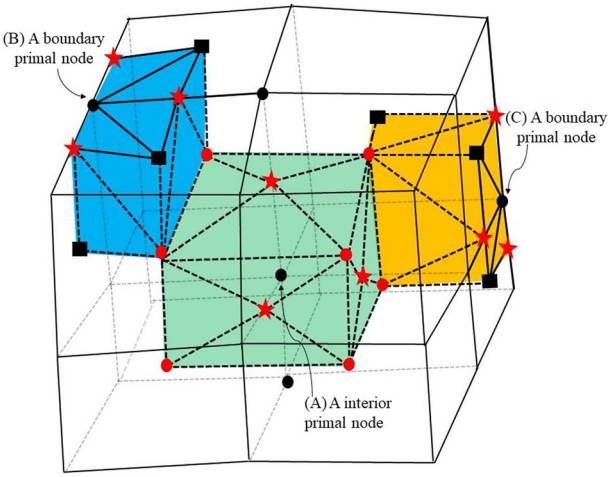

Fig. 4 Dual polygons in dual mesh corresponding to a interior primal node (A, green), two boundary primal nodes (B, blue) and (C, yellow)

Creating mesh points of dual control volumes

Step 8: The mesh point x_M associated with each dual control volume M in $\mathcal{T}_h^*$ will be identified with the primal vertex x_V associated with M if x_V in M, whereas the set $\mathcal{C}^*$ includes two subsets: $\mathcal{C}_\Omega^* = \{x_M \mid x_M \in \Omega\}$ and $\mathcal{C}_{\partial\Omega}^* = \{x_M \mid x_M \in \partial\Omega\}$.

Remark 1 [11, Algorithm 1] of the 3D-SC-FEM method can build triangular dual faces similarly to Algorithm 1 by connecting the vertices of its dual faces to the midpoints of primal edges and the boundary primal nodes. Hence, as mentioned in [11, Remark 3.2], constructing the dual mesh of the EFC-3DFEM method is feasible for real life, complex geometries, as demonstrated in [12, 13].

Remark 2 The dual mesh $\mathcal{T}_h^*$ is a non-overlapping partition of Ω, which is different from the overlapping secondary mesh of the DDFV method (see [7, Remark 1]).

2.3 The subdual tetrahedral mesh

The subdual mesh collection, like the primal and dual meshes, is defined as $\mathcal{D}^{**} = \left(\mathcal{T}_h^{**}, \mathcal{V}^{**}, \mathcal{C}^{**}, \mathcal{E}^{**}, \mathcal{F}^{**}\right)$, where $\mathcal{T}_h^{**}$ is a finite family of tetrahedrons T such that $\bigcup_{T \in \mathcal{T}_h^{**}} \overline{T} = \overline{\Omega}$; $\mathcal{F}^{**}$, $\mathcal{E}^{**}$, and $\mathcal{V}^{**}$ are the faces, edges, and vertices of the mesh $\mathcal{T}_h^{**}$, respectively; $\mathcal{C}^{**}$ is the finite set of tetrahedrons mesh points T in $\mathcal{T}_h^{**}$. By connecting the mesh point x_M of each control volume M in the dual mesh $\mathcal{T}_h^*$ with all of the vertices of its triangular dual faces to produce tetrahedrons (see Fig. 5), we may decompose each control volume M into tetrahedrons and produce the subdual mesh $\mathcal{D}^{**}$.

Remark 3 For actual complex geometries, as seen in [10, 14], the dual mesh $\mathcal{T}_h^*$ can be constructed. Additionally, piecewise linear approximations may be used on universal meshes, thanks to its tetrahedral subdual mesh $\mathcal{T}_h^{**}$.

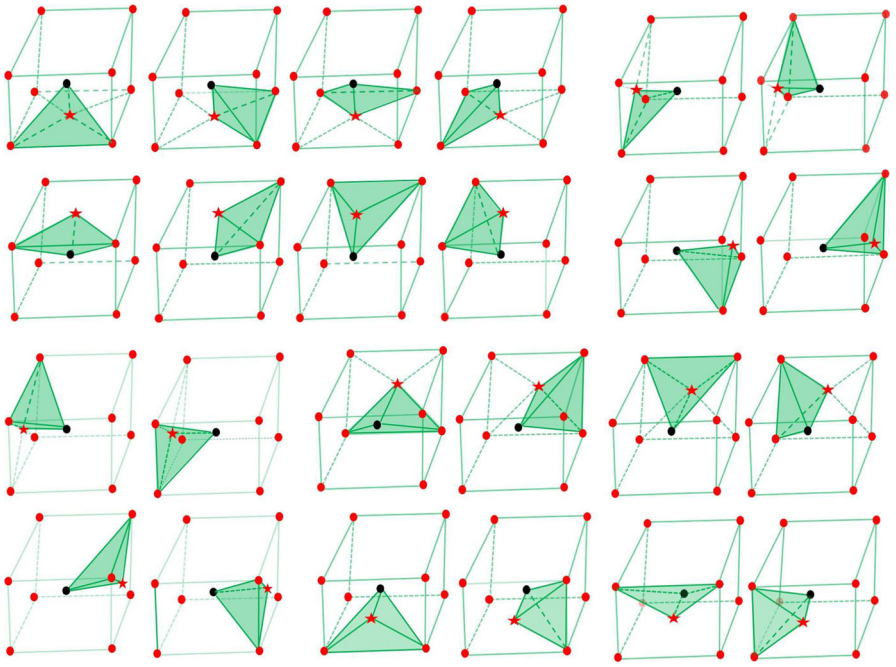

Fig. 5 An illustration of creating tetrahedrons (of the subdual mesh) from a dual control volume: 24 tetrahedrons of the subdual mesh are created from the dual polygon (green) in Fig. 4

Remark 4 By construction of $\mathcal{T}_h^{**}$, we see that

(a) The set $\mathcal{V}^{**}$ only consists of three subsets $\mathcal{C}$, $\mathcal{C}^*$, and $\mathcal{C}_\mathcal{E}$ containing mesh points of the primal mesh, mesh points of the dual mesh, midpoints of primal edges, respectively; $\mathcal{V}^{**} = \mathcal{V}_\Omega^{**} \cup \mathcal{V}_{\partial\Omega}^{**}$ with $\mathcal{V}_\Omega^{**} = \mathcal{C} \cup \mathcal{C}_\Omega^* \cup \mathcal{C}_{\mathcal{E}_\Omega}$, $\mathcal{V}_{\partial\Omega}^{**} = \mathcal{C} \cup \mathcal{C}_{\partial\Omega}^* \cup \mathcal{C}_{\mathcal{E}_{\partial\Omega}}$, and $\mathcal{C}_\mathcal{E} = \mathcal{C}_{\mathcal{E}_\Omega} \cup \mathcal{C}_{\mathcal{E}_{\partial\Omega}}$. Furthermore, for each $M \in \mathcal{T}_h^*$, the set $\mathcal{V}_M^{**}$ of its vertices is defined by

$$\mathcal{V}_M^{**} = \mathcal{C}_M \cup \mathcal{C}_{\mathcal{E}_M} \cup \{x_M\}, \tag{5}$$

where x_M is the mesh point of M, $\mathcal{C}_M = \{x_K \in \mathcal{C} \mid x_K \text{ is a vertex of } M\}$, $\mathcal{E}_M = \{e \in \mathcal{E} \mid x_M \text{ is a vertex of } \mathrm{e}\}$, and $\mathcal{C}_{\mathcal{E}_M} = \{x_\mathrm{e} \in \mathcal{C}_\mathcal{E} \mid \mathrm{e} \in \mathcal{E}_M\}$.

(b) The set $\mathcal{T}_h^{**}$ only has the following subsets:

$$\mathcal{T}_\Omega^{**} := \left\{ T = (x_M x_K x_L x_\mathrm{e}) \in \mathcal{T}_h^{**} \;\middle|\; \begin{array}{l} \mathrm{f} \notin \partial\Omega \;\; \forall \mathrm{f} \in \mathcal{F}_T^{**}, \\ x_M \in \mathcal{C}^*, x_\mathrm{e} \in \mathcal{C}_\mathcal{E} \text{ and } x_K, x_L \in \mathcal{C} \end{array} \right\},$$

$$\mathcal{T}_{\partial\Omega}^{**} := \left\{ T = (x_M x_K x_\mathrm{f} x_\mathrm{e}) \in \mathcal{T}_h^{**} \;\middle|\; \begin{array}{l} \exists \mathrm{f} \in \mathcal{F}_T^{**} \cap \partial\Omega, \\ x_K \in \mathcal{C}, x_M \in \mathcal{C}^*, x_\mathrm{e} \in \mathcal{C}_\mathcal{E} \text{ and } x_\mathrm{f} \in \mathcal{C}_{\mathcal{F}_{\partial\Omega}} \end{array} \right\},$$

where $\mathcal{F}_T^{**}$ is a set of all triangular faces in T.

(c) Each $T = (x_M x_K x_L x_\mathrm{e}) \in \mathcal{T}_\Omega^{**}$ can be partitioned into two sub-tetrahedrons $T_K := (x_M x_K x_\mathrm{f} x_\mathrm{e})$ and $T_L := (x_M x_L x_\mathrm{f} x_\mathrm{e})$, where $\mathrm{f} = \partial K \cap \partial L$, its face point x_f is an intersecting point between a segment $[x_K, x_L]$ and a face f.

Remark 5 Because the subdual mesh $\mathcal{D}^{**}$ is formed by decomposing each control volume M in $\mathcal{T}_h^*$, it satisfies

$$\overline{M} = \bigcup_{T \in \mathcal{T}_{x_M}^{**}} \overline{T}, \tag{6}$$

where x_M is the mesh point of M, and $\mathcal{T}_{x_M}^{**} = \{T \in \mathcal{T}_h^{**} \mid x_M \text{ is a vertex } T\}$. Moreover, for any two different dual elements $M, N \in \mathcal{T}_h^*$ with two mesh points x_M, x_N, we have

$$\mathcal{T}_{x_M}^{**} \cap \mathcal{T}_{x_N}^{**} = \emptyset. \tag{7}$$

Remark 6 In [11], the staggered cell-centered finite element method (SC-FEM) presented the construction of dual and subdual meshes, where the vertices of its subdual mesh include in vertices and mesh points of the primal mesh. By this geometry, the SC-FEM scheme could not imposed the numerical flux continuity. Therefore, the mesh construction of the EFC-3DFEM scheme are absolutely different from the ones of the SC-FEM scheme.

Remark 7 From geometrical construction of the dual and subdual meshes, we observe that each dual control volume $M \in \mathcal{T}_h^*$ is indeed a macro-element-the union of some fixed number of adjacent tetrahedrons of the subdual mesh $\mathcal{T}_h^{**}$ (see [8, pp. 497–498]).

3 The EFC-3DFEM scheme

In this section, we construct the approximate space for the solution $\overline{u}$. On this space, we define the projection and the discrete gradient operators in two cases depending on the characteristics of the tensor Λ. Using these spaces and operators, we may express the discrete version of the problem (4) from which the corresponding linear algebraic systems are derived.

3.1 Spaces and discrete functional characteristics

In order to estimate the solution $\overline{u}$ of (4), the piecewise linear basis functions on the subdual mesh $\mathcal{T}_h^{**}$ and approximations u_P in $\mathbb{R}$ of $u(x_P)$ at nodes x_P in $\mathcal{V}^{**}$ are used. The values $\{u_P\}_{x_P \in \mathcal{V}^{**}}$ are elements of a vector $\mathbf{u}_h$. This vector belongs to the following space:

$$\mathcal{H}_h = \{\mathbf{u}_h := (u_P)_{x_P \in \mathcal{V}^{**}}, \quad u_P \in \mathbb{R}\}. \tag{8}$$

Suppose $h^{**} := \max\left\{h_T = \text{diam}(T),\ \forall T \in \mathcal{T}_h^{**}\right\}$ where h_T is the circumscribed sphere's diameter of the tetrahedral $T \in \mathcal{T}_h^{**}$, if $h \to 0$ then $h^{**} \to 0$.

Since we impose the homogeneous Dirichlet boundary condition (2) (*i.e.*, $u_P = 0$ with $x_P \in \mathcal{V}_{\partial\Omega}^{**}$) on the approximate solution, we need to deal with inner nodes by creating the following subset of $\mathcal{H}_h$

$$\mathcal{H}_h^0 = \{\mathbf{u}_h \in \mathcal{H}_h \ : \ u_P = 0, \quad \forall x_P \in \mathcal{V}_{\partial\Omega}^{**}\}. \tag{9}$$

This space has all basis vectors in $\left\{\mathbf{v}_h^Q\right\}_{x_Q \in \mathcal{V}_\Omega^{**}}$, where each element of a basis vector $\mathbf{v}_h^Q := \left(v_P^Q\right)_{x_P \in \mathcal{V}^{**}}$ is given by $v_P^Q = \begin{cases} 1 & x_P = x_Q, \\ 0 & x_P \neq x_Q, \end{cases}$.

The discrete gradient ∇_Λ and the projection operator Φ must be defined in the following ways on the space $\mathcal{H}_h$ in order to construct the discrete version of (4):

To fulfill the continuity of fluxes across interfaces across primal control volumes, which are specified on each tetrahedron T in $\mathcal{T}_h^{**}$, must take into consideration the tensor Λ (which may be discontinuous in the case where two different approximations of Λ on T are Λ_K on $T \cap K \neq \emptyset$, and Λ_L on $T \cap L \neq \emptyset$, with $L, K \in \mathcal{T}_h$). As a result, their definitions are divided into the following two situations depending on the properties of Λ:

- Case 1. Homogeneous tensors ($\Lambda = \lambda \mathbf{I}$, where $\mathbf{I}$ is the 3D identity tensor, and λ is a positive constant)

For any $\mathbf{u}_h = (u_P)_{x_P \in \mathcal{V}^{**}} \in \mathcal{H}_h^0$ $(i.e.\ u_P = 0, \quad \forall x_P \in \mathcal{V}_{\partial\Omega}^{**})$, we define

$$\Phi \mathbf{u}_h(x) = P_1 \mathbf{u}_h(x) := \sum_{x_P \in \mathcal{V}_\Omega^{**}} u_P L_{1,P}(x), \tag{10}$$

where $L_{1,P}$ is the Lagrange basis function of degree 1 at x_P in $\mathcal{V}_\Omega^{**}$.

Given that $\Phi \mathbf{u}_h(x)$ is a piecewise polynomial of degree 1, the related discrete gradient $\nabla_\Lambda \mathbf{u}_h$ on each T in $\mathcal{T}_h^{**}$ is constant. The restriction of the discrete gradient $\nabla_\Lambda \mathbf{u}_h$ on each T in $\mathcal{T}_h^{**}$ may be written as

$$\begin{aligned}(\nabla_\Lambda \mathbf{u}_h)_T &= \frac{-(u_K - u_M)\mathbf{n}_{(x_M x_L x_\mathfrak{e})} - (u_L - u_M)\mathbf{n}_{(x_M x_K x_\mathfrak{e})} - (u_\mathfrak{e} - u_M)\mathbf{n}_{(x_M x_K x_L)}}{3m_T} \\ &= \frac{-u_K \mathbf{n}_{(x_M x_L x_\mathfrak{e})} - u_L \mathbf{n}_{(x_M x_K x_\mathfrak{e})} - u_M \mathbf{n}_{(x_K x_L x_\mathfrak{e})} - u_\mathfrak{e} \mathbf{n}_{(x_M x_K x_L)}}{3m_T},\end{aligned} \tag{11}$$

with m_T is the volume of the tetrahedron $T = (x_M x_K x_L x_\mathfrak{e})$; $\mathbf{n}_{(x_M x_L x_\mathfrak{e})}$, $\mathbf{n}_{(x_M x_K x_\mathfrak{e})}$, $\mathbf{n}_{(x_K x_L x_\mathfrak{e})}$, and $\mathbf{n}_{(x_M x_K x_L)}$ are four outward normal vectors of T at triangular faces $(x_M x_L x_\mathfrak{e})$, $(x_M x_K x_\mathfrak{e})$, $(x_K x_L x_\mathfrak{e})$, and $(x_M x_K x_L)$, respectively. Their magnitudes are equal to the area of these faces $m_{(x_M x_L x_\mathfrak{e})}$, $m_{(x_M x_K x_\mathfrak{e})}$, $m_{(x_K x_L x_\mathfrak{e})}$, and $m_{(x_M x_K x_L)}$, respectively.

- Case 2: Heterogeneous and anisotropic tensors.

Due to Remark 4.(b), two operators Φ and ∇_Λ will be defined on each $T \in \mathcal{T}_\Omega^{**}$ and $T \in \mathcal{T}_{\partial\Omega}^{**}$.

Let us first consider on each tetrahedron $T := (x_M x_K x_L x_\mathfrak{e}) \in \mathcal{T}_\Omega^{**}$. By Remark 4.(c), the tetrahedron T has two sub-tetrahedrons $T_K = (x_M x_K x_\mathfrak{f} x_\mathfrak{e})$ and $T_L = (x_M x_L x_\mathfrak{f} x_\mathfrak{e})$ with $\mathfrak{f} \in \partial K \cap \partial L$ and its face point $x_\mathfrak{f}$. Remark that T_K, T_L are inside two elements $K, L \in \mathcal{T}_h$, respectively, then the approximation values of Λ

on T_K and T_L are equal to Λ_K and Λ_L, respectively, where $\Lambda_K = \frac{1}{m_K}\int_K \Lambda(x)dx$ and $\Lambda_L = \frac{1}{m_L}\int_L \Lambda(x)dx$. The piecewise linear function $\Phi\mathbf{u}_h(x)$ on T must thus be determined by values at each of vertices of T_K and T_L. To do this, we must propose an auxiliary unknown $u_{\mathtt{f}}^M$ at $x_{\mathtt{f}}$, as follows:

$$\Phi\mathbf{u}_h(x) = \begin{cases} u_M, & x = x_M, \\ u_K, & x = x_K, \\ u_L, & x = x_L, \\ u_{\mathtt{e}}, & x = x_{\mathtt{e}}, \\ u_{\mathtt{f}}^M, & x = x_{\mathtt{f}}. \end{cases} \tag{12}$$

and to define the restrictions of $\nabla_\Lambda \mathbf{u}_h$ by

$$(\nabla_\Lambda \mathbf{u}_h)_{T_K} = \frac{-u_M \mathbf{n}_{(x_K x_{\mathtt{e}} x_{\mathtt{f}})} - u_K \mathbf{n}^K_{(x_M x_{\mathtt{e}} x_{\mathtt{f}})} - u_{\mathtt{e}} \mathbf{n}_{(x_M x_K x_{\mathtt{f}})} - u_{\mathtt{f}}^M \mathbf{n}_{(x_M x_K x_{\mathtt{e}})}}{3m_{T_K}} \quad \text{on } T_K, \tag{13}$$

$$(\nabla_\Lambda \mathbf{u}_h)_{T_L} = \frac{-u_M \mathbf{n}_{(x_L x_{\mathtt{e}} x_{\mathtt{f}})} - u_L \mathbf{n}^L_{(x_M x_{\mathtt{e}} x_{\mathtt{f}})} - u_{\mathtt{e}} \mathbf{n}_{(x_M x_L x_{\mathtt{f}})} - u_{\mathtt{f}}^M \mathbf{n}_{(x_M x_L x_{\mathtt{e}})}}{3m_{T_L}} \quad \text{on } T_L, \tag{14}$$

where $\mathbf{n}^K_{(x_M x_{\mathtt{e}} x_{\mathtt{f}})}$ and $\mathbf{n}^L_{(x_M x_{\mathtt{e}} x_{\mathtt{f}})}$ are the outward vectors of T_K and T_L at triangular face $(x_M x_{\mathtt{e}} x_{\mathtt{f}})$.

In order to fulfill the local continuity of the numerical flux over the triangular face $(x_M x_{\mathtt{e}} x_{\mathtt{f}})$ inside $\mathtt{f}$, the auxiliary unknown $u_{\mathtt{e}}^M$ is selected by

$$\Lambda_K (\nabla_\Lambda \mathbf{u}_h)_{T_K} \cdot \mathbf{n}^K_{(x_M x_{\mathtt{e}} x_{\mathtt{f}})} + \Lambda_L (\nabla_\Lambda \mathbf{u}_h)_{T_L} \cdot \mathbf{n}^L_{(x_M x_{\mathtt{e}} x_{\mathtt{f}})} = 0. \tag{15}$$

Substituting (13) and (14) in (15), it reads

$$\beta_M u_M + \beta_K u_K + \beta_L u_L + \beta_{\mathtt{e}} u_{\mathtt{e}} + \beta_{\mathtt{f}} u_{\mathtt{f}}^M = 0, \tag{16}$$

with

$$\begin{aligned}
\beta_K &= \frac{\left(\Lambda_K \mathbf{n}^K_{(x_M x_{\mathtt{e}} x_{\mathtt{f}})}\right) \cdot \mathbf{n}^K_{(x_M x_{\mathtt{e}} x_{\mathtt{f}})}}{3m_{T_K}}, \quad \beta_L = \frac{\left(\Lambda_L \mathbf{n}^L_{(x_M x_{\mathtt{e}} x_{\mathtt{f}})}\right) \cdot \mathbf{n}^L_{(x_M x_{\mathtt{e}} x_{\mathtt{f}})}}{3m_{T_L}}, \\
\beta_M &= \frac{\left(\Lambda_K \mathbf{n}_{(x_K x_{\mathtt{e}} x_{\mathtt{f}})}\right) \cdot \mathbf{n}^K_{(x_M x_{\mathtt{e}} x_{\mathtt{f}})}}{3m_{T_K}} + \frac{\left(\Lambda_L \mathbf{n}_{(x_L x_{\mathtt{e}} x_{\mathtt{f}})}\right) \cdot \mathbf{n}^L_{(x_M x_{\mathtt{e}} x_{\mathtt{f}})}}{3m_{T_L}}, \\
\beta_{\mathtt{e}} &= \frac{\left(\Lambda_K \mathbf{n}_{(x_M x_K x_{\mathtt{f}})}\right) \cdot \mathbf{n}^K_{(x_M x_{\mathtt{e}} x_{\mathtt{f}})}}{3m_{T_K}} + \frac{\left(\Lambda_L \mathbf{n}_{(x_M x_L x_{\mathtt{f}})}\right) \cdot \mathbf{n}^L_{(x_M x_{\mathtt{e}} x_{\mathtt{f}})}}{3m_{T_L}}, \\
\beta_{\mathtt{f}} &= \frac{\left(\Lambda_K \mathbf{n}_{(x_M x_K x_{\mathtt{e}})}\right) \cdot \mathbf{n}^K_{(x_M x_{\mathtt{e}} x_{\mathtt{f}})}}{3m_{T_K}} + \frac{\left(\Lambda_L \mathbf{n}_{(x_M x_L x_{\mathtt{e}})}\right) \cdot \mathbf{n}^L_{(x_M x_{\mathtt{e}} x_{\mathtt{f}})}}{3m_{T_L}}.
\end{aligned}$$

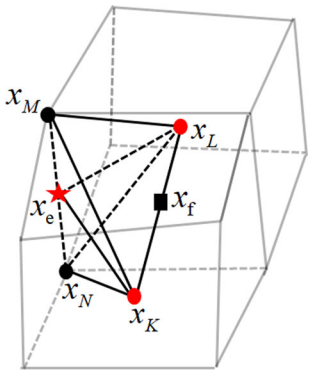

Fig. 6 Two tetrahedrons $T = (x_M x_K x_L x_e)$ and $\widehat{T} = (x_N x_K x_L x_e)$ have the common triangular face $(x_K x_L x_e)$

The above coefficients satisfy

$$\beta_K + \beta_L + \beta_M + \beta_e + \beta_f = 0. \tag{17}$$

From (16), let us mention that all along the paper, we assume that $\beta_f \neq 0$. The linear combination of u_M, u_K, u_L and u_e is provided as the auxiliary unknown u_f^M:

$$u_f^M = \widetilde{\beta}_M^T u_M + \widetilde{\beta}_K^T u_K + \widetilde{\beta}_L^T u_L + \widetilde{\beta}_e^T u_e, \tag{18}$$

with

$$\widetilde{\beta}_K^T = -\frac{\beta_K}{\beta_f}, \quad \widetilde{\beta}_L^T = -\frac{\beta_L}{\beta_f}, \quad \widetilde{\beta}_M^T = -\frac{\beta_M}{\beta_f}, \quad \widetilde{\beta}_e^T = -\frac{\beta_e}{\beta_f}. \tag{19}$$

As a consequence of (17), these above coefficients satisfy

$$\widetilde{\beta}_M^T + \widetilde{\beta}_K^T + \widetilde{\beta}_L^T + \widetilde{\beta}_e^T = 1. \tag{20}$$

Remark 8 Let us consider two tetrahedrons $T := (x_M x_K x_L x_e)$ and $\widehat{T} := (x_N x_K x_L x_e)$ in $\mathcal{T}_h^{**}$, see Fig. 6.

On the tetrahedrons T and $\widehat{T}$, the tensor Λ is heterogeneous and anisotropic, then there exist two auxiliary unknowns given by

$$u_f^M = \widetilde{\beta}_M^T u_M + \widetilde{\beta}_K^T u_K + \widetilde{\beta}_L^T u_L + \widetilde{\beta}_e^T u_e, \tag{21}$$

$$u_f^N = \widetilde{\beta}_N^{\widehat{T}} u_N + \widetilde{\beta}_K^{\widehat{T}} u_K + \widetilde{\beta}_L^{\widehat{T}} u_L + \widetilde{\beta}_e^{\widehat{T}} u_e. \tag{22}$$

Note that $\widetilde{\beta}_N^{\widehat{T}} u_N \neq \widetilde{\beta}_M^T u_M$, thus u_f^M may be different from u_f^N. Consequently, $\Phi \mathbf{u}_h(x)$ is discontinuous at x_f.

Substituting (18) into (13) and (14), the discrete gradient $(\nabla_\Lambda \mathbf{u}_h)_T$ depends on four nodal values u_M, u_K, u_L, and u_e expressed by

$$(\nabla_\Lambda \mathbf{u}_h)_{T_K} = \frac{-u_M \widetilde{\mathbf{n}}_{T_K}^{x_M} - u_K \widetilde{\mathbf{n}}_{T_K}^{x_K} - u_L \widetilde{\mathbf{n}}_{T_K}^{x_L} - u_\mathrm{e} \widetilde{\mathbf{n}}_{T_K}^{x_\mathrm{e}}}{3m_{T_K}}, \tag{23}$$

$$(\nabla_\Lambda \mathbf{u}_h)_{T_L} = \frac{-u_M \widetilde{\mathbf{n}}_{T_L}^{x_M} - u_K \widetilde{\mathbf{n}}_{T_L}^{x_K} - u_L \widetilde{\mathbf{n}}_{T_L}^{x_L} - u_\mathrm{e} \widetilde{\mathbf{n}}_{T_L}^{x_\mathrm{e}}}{3m_{T_L}}, \tag{24}$$

where

$$\begin{aligned}
\widetilde{\mathbf{n}}_{T_K}^{x_M} &= \mathbf{n}_{(x_K x_\mathrm{e} x_\mathrm{f})} + \widetilde{\beta}_M^T \mathbf{n}_{(x_M x_K x_\mathrm{e})}, & \widetilde{\mathbf{n}}_{T_K}^{x_K} &= \mathbf{n}_{(x_M x_\mathrm{e} x_\mathrm{f})}^{x_K} + \widetilde{\beta}_K^T \mathbf{n}_{(x_M x_K x_\mathrm{e})},\\
\widetilde{\mathbf{n}}_{T_K}^{x_\mathrm{e}} &= \mathbf{n}_{(x_M x_K x_\mathrm{f})} + \widetilde{\beta}_\mathrm{e}^T \mathbf{n}_{(x_M x_K x_\mathrm{e})}, & \widetilde{\mathbf{n}}_{T_K}^{x_L} &= \widetilde{\beta}_L^T \mathbf{n}_{(x_M x_K x_\mathrm{e})},\\
\widetilde{\mathbf{n}}_{T_L}^{x_M} &= \mathbf{n}_{(x_L x_\mathrm{e} x_\mathrm{f})} + \widetilde{\beta}_M^T \mathbf{n}_{(x_M x_L x_\mathrm{e})}, & \widetilde{\mathbf{n}}_{T_L}^{x_L} &= \mathbf{n}_{(x_M x_\mathrm{e} x_\mathrm{f})}^{x_L} + \widetilde{\beta}_L^T \mathbf{n}_{(x_M x_L x_\mathrm{e})},\\
\widetilde{\mathbf{n}}_{T_L}^{x_\mathrm{e}} &= \mathbf{n}_{(x_M x_L x_\mathrm{f})} + \widetilde{\beta}_\mathrm{e}^T \mathbf{n}_{(x_M x_L x_\mathrm{e})}, & \widetilde{\mathbf{n}}_{T_L}^{x_K} &= \widetilde{\beta}_K^T \mathbf{n}_{(x_M x_L x_\mathrm{e})},
\end{aligned}$$

and these vectors satisfy

$$\widetilde{\mathbf{n}}_{T_K}^{x_M} + \widetilde{\mathbf{n}}_{T_K}^{x_K} + \widetilde{\mathbf{n}}_{T_K}^{x_\mathrm{e}} + \widetilde{\mathbf{n}}_{T_K}^{x_L} = \mathbf{0}, \quad \widetilde{\mathbf{n}}_{T_L}^{x_M} + \widetilde{\mathbf{n}}_{T_L}^{x_L} + \widetilde{\mathbf{n}}_{T_L}^{x_\mathrm{e}} + \widetilde{\mathbf{n}}_{T_L}^{x_K} = \mathbf{0}, \tag{25}$$

due to (20).

In summary, for any $\mathbf{u}_h \in \mathcal{H}_h$, the piecewise polynomial $\Phi \mathbf{u}_h(x)$ of degree one and the piecewise constant function $\nabla_\Lambda(\mathbf{u}_h)(x)$ are determined on each $T \in \mathcal{T}_\Omega^{**}$ as follows:

$$\Phi_T \mathbf{u}_h(x) = \begin{cases} u_M, & x = x_M,\\ u_K, & x = x_K,\\ u_L, & x = x_L,\\ u_\mathrm{e}, & x = x_\mathrm{e},\\ \widetilde{\beta}_M^T u_M + \widetilde{\beta}_K^T u_K + \widetilde{\beta}_L^T u_L + \widetilde{\beta}_\mathrm{e}^T u_\mathrm{e}, & x = x_\mathrm{f}, \end{cases} \tag{26}$$

$$(\nabla_\Lambda \mathbf{u}_h)_T(x) = \begin{cases} (\nabla_\Lambda \mathbf{u}_h)_{T_K} & \forall x \in T_K,\\ (\nabla_\Lambda \mathbf{u}_h)_{T_L} & \forall x \in T_L, \end{cases} \tag{27}$$

where $(\nabla_\Lambda \mathbf{u}_h)_{T_K}$, $(\nabla_\Lambda \mathbf{u}_h)_{T_L}$ are presented in (23), (24).

For each $T := (x_M x_K x_\mathrm{e} x_\mathrm{f}) \in \mathcal{T}_{\partial\Omega}^{**}$, due to Remark 4.(b), T is inside $K \in \mathcal{T}_h$, as there is only an approximation Λ_K of the tensor Λ on T. Since there is only one approximation tensor Λ_K for Λ on T, the functions $\Phi_T \mathbf{u}_h(x)$ and $(\nabla_\Lambda \mathbf{u}_h)_T(x)$ can be determined by

$$\Phi_T(\mathbf{u}_h)(x) = \sum_{x_P \in \mathcal{V}_T^{**}} u_P L_{1,P}(x), \quad (\nabla_\Lambda \mathbf{u}_h)_T(x) = \sum_{x_P \in \mathcal{V}_T^{**}} u_P \nabla L_{1,P}(x), \quad \forall x \in T, \tag{28}$$

where $\mathcal{V}_T^{**}$ is a set of all vertices of T.

Using the definitions (10), (11), (26), (27), and (28), we formulate the issue (4) in the following discrete form:

$$\text{Finding} \mathbf{u}_h := (u_P)_{x_P \in \mathcal{V}^*} \in \mathcal{H}_h^0, \text{ such that}$$
$$\sum_{T \in \mathcal{T}_h^{**}} \int_T (\Lambda \nabla_\Lambda \mathbf{u}_h) \cdot \nabla_\Lambda \mathbf{v}_h \, dx = \sum_{T \in \mathcal{T}_h^{**}} \int_T f(x) \Phi(\mathbf{v}_h) \, dx, \quad \forall \mathbf{v}_h \in \mathcal{H}_h^0. \tag{29}$$

And we introduce the following definition:

Definition 1 An approximate gradient discretization for the EFC-3DFEM scheme is defined by $(\mathcal{H}_h, h, \Phi, \nabla_\Lambda)$, where

- The set of discrete unknowns $\mathcal{H}_h$ is a finite-dimensional vector space presented in (8).
- The space step h is the maximum positive real circumscribed sphere's diameter for all elements of $\mathcal{T}_h$.
- The mapping $\Phi : \mathcal{H}_h \to L^2(\Omega)$ has the definition of its restriction on each $T \in \mathcal{T}_h^{**}$ presented by (10) for homogeneous tensor Λ case, and by (26) for anisotropic, heterogeneous tensor Λ case.
- The mapping $\nabla_\Lambda : \mathcal{H}_h \to L^2(\Omega)^3$ has the definition of its restriction on each $T \in \mathcal{T}_h^{**}$ presented by (11) for homogeneous tensor Λ case, and by (27) for anisotropic, heterogeneous tensor Λ case.

3.2 The algebraic system of the EFC-3DFEM scheme

To construct the system of linear equations from the discrete problem (29), we continue by selecting its test vectors $\mathbf{v}_h$ as basis vectors $\mathbf{v}_h^Q$ of $\mathcal{H}_h^0$ with x_Q in $\mathcal{V}_\Omega^{**}$ in two steps:

Step 1. For each $x_M \in \mathcal{C}_\Omega^* \subset \mathcal{V}_\Omega^{**}$, we take $\mathbf{v}_h = \mathbf{v}_h^M$ in (29). Due to Remark 5, two sets $\text{supp}\{\Phi(\mathbf{v}_h^M)\}$, $\text{supp}\{\nabla_\Lambda \mathbf{v}_h^M\}$ belong to M. Thus, (29) can be rewritten as

$$\sum_{T \in \mathcal{T}_{x_M}^{**}} \int_T (\Lambda \nabla_\Lambda \mathbf{u}_h) \cdot \nabla_\Lambda \mathbf{v}_h^M \, dx = \sum_{T \in \mathcal{T}_{x_M}^{**}} \int_T f(x) \Phi(\mathbf{v}_h^M) \, dx. \tag{30}$$

By (5), all unknowns in (30) consist only of u_M, $\{u_K, \ x_K \in \mathcal{C}_M\}$ and $\{u_\epsilon, \ \epsilon \in \mathcal{E}_M\}$.
Therefore, the computational process can be expressed by the following system in matrix form:

$$\mathscr{M}\mathbf{U}^* + \mathscr{K}^*\mathbf{U} = \mathscr{F}^*, \tag{31}$$

where $\mathbf{U}^* = (u_M)_{x_M \in \mathcal{C}_\Omega^*} \in \mathbb{R}^{|\mathcal{C}_\Omega^*|}$, the notation $|\mathcal{C}_\Omega^*|$ represents the cardinality of set $\mathcal{C}_\Omega^*$, and $\mathbf{U} = (u_P)_{x_P \in (\mathcal{C} \cup \mathcal{C}_{\mathcal{E}_\Omega})} \in \mathbb{R}^d$. The diagonal matrix $\mathscr{M} \in \mathbb{R}^{|\mathcal{C}_\Omega^*| \times |\mathcal{C}_\Omega^*|}$ has each diagonal element equal to $\sum_{T \in \mathcal{T}_{x_M}^{**}} \int_T \left(\Lambda \nabla_\Lambda \mathbf{v}_h^M\right) \cdot$

$\nabla_\Lambda \mathbf{v}_h^M \, dx$, with $x_M \in \mathcal{C}_\Omega^*$. The matrix $\boldsymbol{\mathscr{K}}^* \in \mathbb{R}^{|\mathcal{C}_\Omega^*| \times d}$ has each component determined by $\sum_{T \in \mathcal{T}_{x_M}^{**}} \int_T \left(\Lambda \nabla_\Lambda \mathbf{v}_h^P\right) \cdot \nabla_\Lambda \mathbf{v}_h^M \, dx$, with $d = (|\mathcal{C}| + |\mathcal{E}_\Omega|)$, $x_M \in \mathcal{C}_\Omega^*$, and $x_P \in \mathcal{C}_M \cup \mathcal{C}_{\mathcal{E}_M}$. The vector $\boldsymbol{\mathscr{F}}^*$ is equal to $\left(\sum_{T \in \mathcal{T}_{x_M}^{**}} \int_T f(x)\Phi(\mathbf{v}_h^M) \, dx\right)_{x_M \in \mathcal{C}_\Omega^*}$. The system (31) leads to

$$\mathbf{U}^* = \boldsymbol{\mathscr{M}}^{-1}\boldsymbol{\mathscr{F}}^* - \boldsymbol{\mathscr{M}}^{-1}\boldsymbol{\mathscr{K}}^*\mathbf{U}, \tag{32}$$

which means that, for each $x_M \in \mathcal{C}_\Omega^*$, the unknown u_M can be expressed as a combination of $\{u_K\}_{x_K \in \mathcal{C}_M}$, $\{u_\mathrm{e}\}_{\mathrm{e} \in \mathcal{E}_\Omega}$, and the source term f.

Step 2. For each $x_K \in \mathcal{C} \subset \mathcal{V}_\Omega^{**}$ and $x_\mathrm{e} \in \mathcal{C}_\mathcal{E} \subset \mathcal{V}_\Omega^{**}$, by taking $\mathbf{v}_h = \mathbf{v}_h^K$ and $\mathbf{v}_h = \mathbf{v}_h^\mathrm{e}$, (29) can be rewritten as

$$\sum_{T \in \mathcal{T}_{x_K}^{**}} \int_T (\Lambda \nabla_\Lambda \mathbf{u}_h) \cdot \nabla_\Lambda \mathbf{v}_h^K \, dx = \sum_{T \in \mathcal{T}_{x_K}^{**}} \int_T f(x)\Phi(\mathbf{v}_h^K) \, dx, \tag{33}$$

$$\sum_{T \in \mathcal{T}_{x_\mathrm{e}}^{**}} \int_T (\Lambda \nabla_\Lambda \mathbf{u}_h) \cdot \nabla_\Lambda \mathbf{v}_h^\mathrm{e} \, dx = \sum_{T \in \mathcal{T}_{x_\mathrm{e}}^{**}} \int_T f(x)\Phi(\mathbf{v}_h^\mathrm{e}) \, dx, \tag{34}$$

where

$$\mathcal{T}_{x_K}^{**} := \left\{T \in \mathcal{T}_h^{**} \mid T \text{ has a vertex } x_K\right\},$$

$$\mathcal{T}_{x_\mathrm{e}}^{**} := \left\{T \in \mathcal{T}_h^{**} \mid T \text{ has a vertex } x_\mathrm{e}\right\}.$$

Similar as Step 1, the computational process is also presented by the following matrix form as

$$\boldsymbol{\mathscr{M}}^*\mathbf{U}^* + \boldsymbol{\mathscr{K}}\mathbf{U} = \boldsymbol{\mathscr{F}}, \tag{35}$$

where $d = (|\mathcal{C}| + |\mathcal{E}_\Omega|)$, the vector $\boldsymbol{\mathscr{F}} \in \mathbb{R}^d$, and two matrices $\boldsymbol{\mathscr{M}}^* \in \mathbb{R}^{d \times |\mathcal{C}_\Omega^*|}$, $\boldsymbol{\mathscr{K}} \in \mathbb{R}^{d \times d}$.
Substituting (32) into (35), it implies

$$\mathbf{A} \cdot \mathbf{U} = \mathbf{F}, \tag{36}$$

with $\mathbf{A} = \boldsymbol{\mathscr{K}} - \boldsymbol{\mathscr{M}}^*\boldsymbol{\mathscr{M}}^{-1}\boldsymbol{\mathscr{K}}^* \in \mathbb{R}^{d \times d}$, $\mathbf{F} = \boldsymbol{\mathscr{F}} - \boldsymbol{\mathscr{M}}^*\boldsymbol{\mathscr{M}}^{-1}\boldsymbol{\mathscr{F}}^* \in \mathbb{R}^d$, $\mathbf{U} = (u_P)_{x_P \in (\mathcal{C} \cup \mathcal{C}_{\mathcal{E}_\Omega})} \in \mathbb{R}^d$. Note that the system (36) only depends on the unknowns of $\{u_K\}_{x_K \in \mathcal{C}}$ and $\{u_\mathrm{e}\}_{\mathrm{e} \in \mathcal{E}_\Omega}$, therefore the proposed scheme is called the edge-cell finite element scheme.

Remark 9 If the homogeneous Dirichlet boundary condition (2) is replaced by a Neumann or Robin boundary condition, the EFC-3DFEM scheme must have the additional unknowns $\{u_\mathrm{e}\}_{\mathrm{e} \in \mathcal{E}_{\partial\Omega}}$, $\{u_\mathrm{f}\}_{\mathrm{f} \in \mathcal{F}_{\partial\Omega}}$, and $\{u_Q\}_{x_Q \in \mathcal{C}_{\partial\Omega}^*}$.

It is now necessary to demonstrate the existence and originality of the solution for (36) where the stiffness matrix $\mathbf{A}$ is a symmetric positive definite matrix. The exact claim reads as follows:

Proposition 1 *The stiffness matrix* $\mathbf{A}$ *in (36) is symmetric and positive definite.*

Proof When the tensor Λ is isotropic, (10) and (11) show that the EFC-3DFEM is equivalent to the standard finite element on the tetrahedral subdual mesh $\mathcal{T}_h^{**}$. Thus, the stiffness matrix $\mathbf{A}$ is always symmetric and positive definite.

For the heterogeneous and anisotropic tensor Λ case, due to the Schur complement property (see [15, Theorem 1.12, p. 34]), it helps to notice that if the matrix $\mathbf{S} = \begin{pmatrix} \mathscr{M} & \mathscr{K}^* \\ \mathscr{M}^* & \mathscr{K} \end{pmatrix}$ is symmetric and positive definite, then the matrix $\mathbf{A} := \mathscr{K} - \mathscr{M}^* \mathscr{M}^{-1} \mathscr{K}^* \in \mathbb{R}^{d\times d}$ is also symmetric and positive definite.

Obviously, we verify that $\mathbf{S}$ is symmetric, since we have the symmetric tensor Λ and the following result for any $\mathbf{u}_h = (u_P)_{x_P \in \mathcal{V}_\Omega^{**}}$, $\mathbf{v}_h = (v_P)_{x_P \in \mathcal{V}_\Omega^{**}} \in \mathcal{H}_h^0$

$$\widehat{\mathbf{U}}^T \mathbf{S} \widehat{V} = \sum_{T \in \mathcal{T}_h^{**}} \int_T \Lambda \nabla_\Lambda \mathbf{u}_h \cdot \nabla_\Lambda \mathbf{v}_h \, dx = \sum_{T \in \mathcal{T}_h^{**}} \int_T \Lambda \nabla_\Lambda \mathbf{v}_h \cdot \nabla_\Lambda \mathbf{u}_h \, dx = \widehat{V}^T \mathbf{S} \widehat{\mathbf{U}}, \tag{37}$$

where $\widehat{\mathbf{U}} = \begin{pmatrix} \mathbf{U}^* \\ \mathbf{U} \end{pmatrix}$, $\widehat{V} = \begin{pmatrix} V^* \\ V \end{pmatrix}$, $\mathbf{U}^* = (u_M)_{x_M \in \mathcal{C}_\Omega^*}$, ${x_V}^* = (v_M)_{x_M \in \mathcal{C}_\Omega^*}$, $\mathbf{U} = (u_P)_{x_P \in (\mathcal{C} \cup \mathcal{C}_{\mathcal{E}_\Omega})}$ and $x_V = (v_P)_{x_P \in (\mathcal{C} \cup \mathcal{C}_{\mathcal{E}_\Omega})}$. Note that $\mathcal{V}_\Omega^{**} = \left(\mathcal{C}_\Omega^* \cup \mathcal{C} \cup \mathcal{C}_{\mathcal{E}_\Omega}\right)$ due to Remark 4 (a).

To verify the positive definite property of $\mathbf{S}$, we need to prove that

$$\widehat{\mathbf{U}}^T \mathbf{S} \widehat{\mathbf{U}} = \sum_{T \in \mathcal{T}_h^{**}} \int_T \Lambda \nabla_\Lambda \mathbf{u}_h \cdot \nabla_\Lambda \mathbf{u}_h \, dx > 0, \tag{38}$$

for any $\mathbf{u}_h \in \mathcal{H}_h^0$ such that $\mathbf{u}_h \neq 0$.

From the property (3), the right-hand side of (38) can be estimated by

$$\sum_{T \in \mathcal{T}_h^{**}} \int_T \Lambda \nabla_\Lambda \mathbf{u}_h \cdot \nabla_\Lambda \mathbf{u}_h \, dx \geq \underline{\lambda} \sum_{T \in \mathcal{T}_h^{**}} \int_T \nabla_\Lambda \mathbf{u}_h \cdot \nabla_\Lambda \mathbf{u}_h \, dx, \tag{39}$$

in which $\int_T \nabla_\Lambda \mathbf{u}_h \cdot \nabla_\Lambda \mathbf{u}_h \, dx \geq 0$ for all $T \in \mathcal{T}_h^{**}$. Moreover, since $\mathbf{u}_h \neq 0$ and $\mathbf{u}_h \in \mathcal{H}_h^0$ (*i.e.*, $u_P = 0, \quad \forall x_P \in \mathcal{V}_{\partial\Omega}^{**}$), we always have at least one tetrahedron T_0 satisfying one of the following two cases:

Case 1. With $T_0 := (x_M x_K x_{\mathtt{e}} x_{\mathtt{f}}) \in \mathcal{T}_{\partial\Omega}^{**}$, we use (11) and values $u_{\mathtt{e}} = u_{\mathtt{f}} = 0$ at $x_{\mathtt{e}}, x_{\mathtt{f}} \in \partial\Omega$ to compute

$$\underline{\lambda} \int_{T_0} \nabla_\Lambda \mathbf{u}_h \cdot \nabla_\Lambda \mathbf{u}_h \, dx$$

$$= \frac{\underline{\lambda}}{9m_T} \begin{cases} \left(u_M \mathbf{n}_{(x_K x_e x_f)} + u_K \mathbf{n}_{(x_M x_e x_f)}\right)^2 > 0, & \text{if } u_M, u_K \neq 0, \\ \left(u_M \mathbf{n}_{(x_K x_e x_f)}\right)^2 > 0, & \text{if } u_M \neq 0, \\ \left(u_K \mathbf{n}_{(x_M x_e x_f)}\right)^2 > 0, & \text{if } u_K \neq 0, \end{cases} \tag{40}$$

where $\left(u_M \mathbf{n}_{(x_K x_e x_f)} + u_K \mathbf{n}_{(x_M x_e x_f)}\right) \neq \mathbf{0}$ if $u_M, u_K \neq 0$.

Case 2. With $T_0 := (x_M x_K x_L x_e) \in \mathcal{T}_\Omega^{**}$ having two sub-tetrahedrons $T_{0,K} = (x_M x_K x_e x_f)$ and $T_{0,L} = (x_M x_L x_e x_f)$, we use (27) to compute

$$\underline{\lambda} \int_{T_0} \nabla_\Lambda \mathbf{u}_h \cdot \nabla_\Lambda \mathbf{u}_h \, dx = \frac{\underline{\lambda}}{9m_{T_{0,K}}} \left(\boldsymbol{I}_{T_0}^{(1)}\right)^2 + \frac{\underline{\lambda}}{9m_{T_{0,L}}} \left(\boldsymbol{I}_{T_0}^{(2)}\right)^2,$$

where

$$\boldsymbol{I}_{T_0}^{(1)} = \left(u_M \widetilde{\mathbf{n}}_{T_K}^{x_M} + u_K \widetilde{\mathbf{n}}_{T_K}^{x_K} + u_L \widetilde{\mathbf{n}}_{T_K}^{x_L} + u_e \widetilde{\mathbf{n}}_{T_K}^{x_e}\right),$$
$$\boldsymbol{I}_{T_0}^{(2)} = \left(u_M \widetilde{\mathbf{n}}_{T_L}^{x_M} + u_K \widetilde{\mathbf{n}}_{T_L}^{x_K} + u_L \widetilde{\mathbf{n}}_{T_L}^{x_L} + u_e \widetilde{\mathbf{n}}_{T_L}^{x_e}\right).$$

Obviously, the two vectors $\boldsymbol{I}_{T_0}^{(1)}$ and $\boldsymbol{I}_{T_0}^{(2)}$ are different from $\mathbf{0}$, since we have the property (25), and the set $\{u_M, u_K, u_L, u_e\}$ satisfies at most three non-zero elements and at least one element equal to 0. Therefore, we get

$$\underline{\lambda} \int_{T_0} \nabla_\Lambda \mathbf{u}_h \cdot \nabla_\Lambda \mathbf{u}_h \, dx > 0. \tag{41}$$

Owning to (39)–(41), we obtain

$$\widehat{\mathbf{U}}^T \mathbf{S} \widehat{\mathbf{U}} \geq \underline{\lambda} \sum_{T \in \mathcal{T}_h^{**}} \int_T \nabla_\Lambda \mathbf{u}_h \cdot \nabla_\Lambda \mathbf{u}_h \, dx \geq \underline{\lambda} \int_{T_0} \nabla_\Lambda \mathbf{u}_h \cdot \nabla_\Lambda \mathbf{u}_h \, dx > 0. \tag{42}$$

This ends the proof of Proposition 1. □

4 Convergence analysis

When applied to the isotropic tensor situation, the EFC-3DFEM method is similar to the traditional Finite Element Method (FEM) based on first-order Lagrange basis functions on $\mathcal{T}_h^{**}$, and convergence is always ensured.

We study here the convergence of the EFC-3DFEM method for the anisotropic and heterogeneous tensor situation (possibly discontinuous). This work begins by introducing the following two operators: $S_h : C_c^\infty(\Omega) \to \mathbb{R}$ and $W_h : \left(C_c^\infty(\Omega)\right)^3 \to \mathbb{R}$ defined by

$$S_h(\varphi) = \left[\|\Phi(\boldsymbol{\varphi}_h) - \varphi\|_{L^2(\Omega)}^2 + \|\nabla_\Lambda \boldsymbol{\varphi}_h - \nabla\varphi\|_{L^2(\Omega)}^2\right]^{1/2},$$

$$\text{with } \varphi \in C_c^\infty(\Omega),\ \boldsymbol{\varphi}_h := (\varphi(x_P))_{x_P \in \mathcal{V}^{**}} \in \mathcal{H}_h^0,$$

$$\text{and } W_h(\boldsymbol{\varphi}) = \max_{\mathbf{v}_h \in \mathcal{H}_h \setminus \{\mathbf{0}\}} \frac{1}{\|\nabla_\Lambda \mathbf{v}_h\|_{\left(L^2(\Omega)\right)^3}} \int_\Omega [\nabla_\Lambda \mathbf{v}_h \cdot \boldsymbol{\varphi} + \Phi(\mathbf{v}_h)\,\mathrm{div}(\boldsymbol{\varphi})]\,dx,$$

$$\text{with } \boldsymbol{\varphi} \in \left(C_c^\infty(\Omega)\right)^3.$$

As consequence of [16, Lemma 2.2 and Corollary 2.3], if the EFC-3DFEM scheme satisfies the strong consistency

$$\lim_{h \to 0} S_h(\varphi) = 0, \quad \forall \varphi \in C_c^\infty(\Omega), \tag{43}$$

the dual consistency

$$\lim_{h \to 0} W_h(\boldsymbol{\varphi}) = 0, \quad \forall \boldsymbol{\varphi} \in \left(C_c^\infty(\Omega)\right)^3, \tag{44}$$

and the coercive property, *i.e.*, there exists a positive constant C independent of h, such that

$$\|\Phi \mathbf{v}_h\|_{L^2(\Omega)} \leq C \|\nabla_\Lambda \mathbf{v}_h\|_{\left(L^2(\Omega)\right)^3}, \quad \forall \mathbf{v}_h \in \mathcal{H}_h, \tag{45}$$

then its convergence is verified, and

$$\|\nabla \overline{u} - \nabla_\Lambda \mathbf{u}_h\|_{\left(L^2(\Omega)\right)^3} \to 0, \quad \text{as } h \to 0, \tag{46}$$

$$\|\overline{u} - \Phi \mathbf{u}_h\|_{L^2(\Omega)} \to 0, \quad \text{as } h \to 0. \tag{47}$$

Next, rather than proving the strong, dual consistencies (43), (44) and the coercive property directly, this work simplifies the process by checking these properties for a variant form of the EFC-3DFEM scheme, referred to as the EFC-3DFEMb scheme. The description of this scheme is as follows:

Finding$\mathbf{u}_h \in \mathcal{H}_h^0$such that

$$\sum_{T \in \mathcal{T}_h^{**}} \int_T (\Lambda \nabla_\Lambda \mathbf{u}_h) \cdot \nabla_\Lambda \mathbf{v}_h \, dx = \sum_{T \in \mathcal{T}_h^{**}} \int_T f(x) P_1 \mathbf{v}_h \, dx, \quad \forall \mathbf{v}_h := (v_P)_{x_P \in \mathcal{V}^{**}} \in \mathcal{H}_h^0, \tag{48}$$

where the polynomial $P_1 \mathbf{v}_h$ represents a first-order Lagrange basis function on the subdual mesh $\mathcal{T}_h^{**}$, with a value $P_1 \mathbf{v}_h(x_P) = v_P$ assigned at each point $x_P \in \mathcal{V}^{**}$.

In the purpose of presenting the proof for the convergence of the EFC-3DFEMb scheme, we need to introduce the following definitions and notations:

Definition 2 An approximate gradient discretization for the EFC-3DFEMb scheme is defined by $(\mathcal{H}_h, h, P_1, \nabla_\Lambda)$, where

- The set of discrete unknowns $\mathcal{H}_h$ is a finite-dimensional vector space presented in (8).

- The space step h is the maximum positive real circumscribed sphere's diameter for all elements of $\mathcal{T}_h$.
- the mapping $P_1 : \mathcal{H}_h \to L^2(\Omega)$ is a first-order Lagrange basis functions on subdual mesh $\mathcal{T}_h^{**}$, with $\mathbf{v}_h = (v_P)_{x_P \in \mathcal{V}^{**}} \in \mathcal{H}_h$, and a value $P_1\mathbf{v}_h(x_P) = v_P$ assigned at each point $x_P \in \mathcal{V}^{**}$.
- The mapping $\nabla_\Lambda : \mathcal{H}_\mathcal{D} : \mathcal{H}_h \to L^2(\Omega)^3$ has the definition of its restriction on each $T \in \mathcal{T}_h^{**}$ presented by (11) for homogeneous tensor Λ case, and by (27) for anisotropic, heterogeneous tensor Λ case.

The dual and strong consistencies for the EFC-3DFEMb scheme are evidenced by their properties measured through the following operators $\widehat{S}_h$ and $\widehat{W}_h$ as outlined below:

$$\widehat{S}_h(\varphi) = \left[\| P_1\boldsymbol{\varphi}_h - \varphi\|^2_{L^2(\Omega)} + \|\nabla_\Lambda\boldsymbol{\varphi}_h - \nabla\varphi\|^2_{(L^2(\Omega))^3} \right]^{1/2}, \forall\varphi \in C_c^\infty(\Omega), \quad (49)$$

with $\boldsymbol{\varphi}_h := (\varphi(x_P))_{x_P \in \mathcal{V}^{**}} \in \mathcal{H}_h^0$, and for all $\boldsymbol{\varphi} \in \left(C_c^\infty(\Omega)\right)^3$

$$\widehat{W}_h(\boldsymbol{\varphi}) = \max_{\mathbf{v}_h \in \mathcal{H}_h \setminus \{\mathbf{0}\}} \frac{1}{\|\nabla_\Lambda \mathbf{v}_h\|_{(L^2(\Omega))^3}} \int_\Omega [\nabla_\Lambda \mathbf{v}_h \cdot \boldsymbol{\varphi} + P_1\mathbf{v}_h \operatorname{div}(\boldsymbol{\varphi})]\, dx. \quad (50)$$

By utilizing the results presented in (70) and (71) from Proposition 2, along with Corollary 1, it can be demonstrated that the EFC-3DFEM scheme also satisfies the strong and dual consistency properties for the anisotropic and heterogeneous tensor situation (potentially discontinuous).

Let us now prove that the EFC-3DFEMb scheme satisfies the strong, dual consistency, and coercive properties. For given operators Φ and ∇_Λ specified on each tetrahedron T in $\mathcal{T}_h^{**}$ as described in Sect. 3, we need to define the following subsets of $\mathcal{T}_h^{**}$ in relation to the tensor Λ:

$$\mathcal{T}_{\text{const}}^{**} = \left\{ T \in \mathcal{T}_h^{**} \mid \Lambda(x) \text{ is constant on } T \right\},$$
$$\mathcal{T}_{\Lambda}^{**} = \left\{ T \in \mathcal{T}_h^{**} \mid \Lambda(x) \text{ is discontinuous on } T \right\}.$$

For any tetrahedron $T := (x_M x_K x_L x_\mathrm{e}) \in \mathcal{T}_h^{**} \setminus \mathcal{T}_{\text{const}}^{**}$, it has two sub-tetrahedrons $T_K := (x_M x_K x_\mathrm{e} x_\mathrm{f})$ and $T_L := (x_M x_L x_\mathrm{e} x_\mathrm{f})$, see Fig. 7.

In addition, we need to introduce the following geometrical notations used in lemmas and theorems:

(i) The sets $\mathcal{V}_T^{(1)}$, $\mathcal{V}_T^{(2)}$, and $\mathcal{V}_T^{(3)}$ contain pairs and triples of vertices that can be defined as

$$\mathcal{V}_T^{(1)} = \{x_M, x_K, x_L, x_\mathrm{e}\},$$
$$\mathcal{V}_T^{(2)} = \{(x_M, x_K), (x_M, x_L), (x_M, x_\mathrm{e}), (x_K, x_L), (x_K, x_\mathrm{e}), (x_L, x_\mathrm{e})\},$$
$$\mathcal{V}_T^{(3)} = \{(x_M, x_K, x_L), (x_M, x_L, x_\mathrm{e}), (x_M, x_K, x_\mathrm{e}), (x_K, x_L, x_\mathrm{e})\}.$$

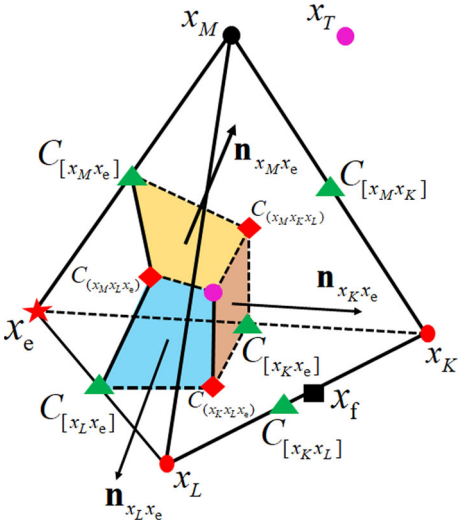

Fig. 7 A tetrahedron $T = (x_M x_K x_L x_e)$ with four vertices $x_M \in \mathcal{C}^*$, $x_K, x_L \in \mathcal{C}$, and an edge point x_e with $e \in \mathcal{E}_\Omega$

(ii) For each pair $(x_N, x_Q) \in \mathcal{V}_T^{(2)}$, the notation $[x_N x_Q]$ represents an edge, with its midpoint denoted as $C_{[x_N x_Q]}$ and its length as $m_{[x_N x_Q]}$.

(iii) For each triple $(x_N, x_Q, x_R) \in \mathcal{V}_T^{(3)}$, the notation $(x_N x_Q x_R)$ is a triangular face, with its centroid denoted as $C_{(x_N x_Q x_R)}$, and its area as $m_{(x_N x_Q x_R)}$.

(iv) For a point $x_N \in \mathcal{V}_T^{(1)}$ and a triple $(x_Q, x_R, x_S) \in \mathcal{V}_T^{(3)}$, $d^{x_N}_{(x_Q x_R x_S)}$ is the distance from x_N to the face $(x_Q x_R x_S)$.

(v) The point x_T is the centroid of the tetrahedron T.

(vi) The following notations

$$
\begin{aligned}
\mathtt{f}_{[x_M x_e]} &= \left(x_T, C_{[x_M x_e]}, C_{(x_M x_K x_e)}, C_{(x_M x_L x_e)}\right),\\
\mathtt{f}_{[x_K x_e]} &= \left(x_T, C_{[x_K x_e]}, C_{(x_M x_K x_e)}, C_{(x_K x_L x_e)}\right),\\
\mathtt{f}_{[x_L x_e]} &= \left(x_T, C_{[x_L x_e]}, C_{(x_M x_L x_e)}, C_{(x_K x_L x_e)}\right),\\
\mathtt{f}_{[x_M x_K]} &= \left(x_T, C_{[x_M x_K]}, C_{(x_M x_K x_e)}, C_{(x_M x_K x_L)}\right),\\
\mathtt{f}_{[x_M x_L]} &= \left(x_T, C_{[x_M x_L]}, C_{(x_M x_L x_e)}, C_{(x_M x_K x_L)}\right),\\
\mathtt{f}_{[x_K x_L]} &= \left(x_T, C_{[x_K x_L]}, C_{(x_M x_K x_L)}, C_{(x_K x_L x_e)}\right),
\end{aligned}
$$

are six quadrangular faces constructed by connecting the centroid x_T to centroids on boundary triangular faces and edges of T.

(vii) Using the above faces, the vertices x_M, x_K, x_L, and x_e involved in $\left\{\mathtt{f}_{[x_M x_e]}, \mathtt{f}_{[x_K x_e]}, \mathtt{f}_{[x_L x_e]}\right\}$, $\left\{\mathtt{f}_{[x_M x_K]}, \mathtt{f}_{[x_K x_e]}, \mathtt{f}_{[x_K x_L]}\right\}$, $\left\{\mathtt{f}_{[x_M x_L]}, \mathtt{f}_{[x_L x_e]}, \mathtt{f}_{[x_K x_L]}\right\}$, and $\left\{\mathtt{f}_{[x_M x_e]}, \mathtt{f}_{[x_L x_e]}, \mathtt{f}_{[x_K x_e]}\right\}$ are connected in order to form the polygons P_{x_M}, P_{x_K}, P_{x_L}, and P_{x_e}, respectively. These polygons lie in the tetrahedron T and satisfy

$$
\overline{T} = \overline{P}_{x_M} \cup \overline{P}_{x_K} \cup \overline{P}_{x_L} \cup \overline{P}_{x_e}.
$$

(viii) For each pair $(x_N, x_Q) \in \mathcal{V}_T^{(2)}$, the polygon P_{x_N} has the outward normal vector $\mathbf{n}_{x_N x_Q}$ at $\mathtt{f}_{[x_N x_Q]} \equiv \mathtt{f}_{[x_Q x_N]}$. The vector $\mathbf{n}_{x_N x_Q}$ has a magnitude $\left|\mathbf{n}_{x_N x_Q}\right|$ equal to the area $m_{\mathtt{f}_{[x_N x_Q]}}$ and also satisfies $\mathbf{n}_{x_N x_Q} = -\mathbf{n}_{x_Q x_N}$.

(ix) For each pair $(x_N, x_Q) \in \mathcal{V}_T^{(2)}$, $d_{x_N x_Q}$ is the distance from $x_N \in \mathcal{V}_T^{(1)}$ to the face $\mathtt{f}_{[x_N x_Q]}$, and it satisfies $d_{x_N x_Q} = d_{x_Q x_N}$.

(x) Besides, we introduce an operator Π_h^0 defined on $\mathcal{H}_h$, specifically as follows: for any $\mathbf{u}_h \in \mathcal{H}_h$, on each $T = (x_M x_K x_L x_\mathtt{e})$, $\Pi_h^0(\mathbf{u}_h)$ is a characteristic function such that

$$\Pi_h^0(\mathbf{u}_h(x)) = \begin{cases} u_M & \text{if } x \in P_{x_M}, \\ u_K & \text{if } x \in P_{x_K}, \\ u_L & \text{if } x \in P_{x_L}, \\ u_\mathtt{e} & \text{if } x \in P_{x_\mathtt{e}}. \end{cases} \tag{51}$$

(xi) To estimate the convergence, $\mathcal{H}_h$ is endowed with the norm

$$\|\mathbf{u}_h\|_{1,\mathcal{T}_h^{**}}^2 = \sum_{\substack{\in \mathcal{T}_h^{**} \\ T:=(x_M x_K x_L x_\mathtt{e})}} \left[\begin{array}{l} \frac{|\mathbf{n}_{x_M x_K}|}{d_{x_M x_K}}(u_K - u_M)^2 + \frac{|\mathbf{n}_{x_M x_L}|}{d_{x_M x_L}}(u_L - u_M)^2 \\ + \frac{|\mathbf{n}_{x_M x_\mathtt{e}}|}{d_{x_M x_\mathtt{e}}}(u_\mathtt{e} - u_M)^2 + \frac{|\mathbf{n}_{x_K x_L}|}{d_{x_K x_L}}(u_L - u_K)^2 \\ + \frac{|\mathbf{n}_{x_K x_\mathtt{e}}|}{d_{x_K x_\mathtt{e}}}(u_\mathtt{e} - u_K)^2 + \frac{|\mathbf{n}_{x_L x_\mathtt{e}}|}{d_{x_L x_\mathtt{e}}}(u_\mathtt{e} - u_L)^2 \end{array} \right]. \tag{52}$$

The next step is to examine the characteristics of the discrete gradient ∇_Λ as follows:

Lemma 1 *For $(\mathcal{H}_h, h, P_1, \nabla_\Lambda)$ being a family of discretizations in the sense of Definition 2, which satisfies the below assumptions: for any $T := (x_M x_K x_L x_\mathtt{e}) \in \mathcal{T}_h^{**} \backslash (\mathcal{T}_\Lambda^{**} \cup \mathcal{T}_{\text{const}}^{**})$, there exists a positive constant δ independent of h, such that*

Assumption A1 $$\frac{\min\left\{d_{(x_M x_\mathtt{e} x_\mathtt{f})}^{x_K}, d_{(x_M x_\mathtt{e} x_\mathtt{f})}^{x_L}, d_{(x_K x_L x_\mathtt{e})}^{x_M}, d_{(x_M x_K x_L)}^{x_\mathtt{e}}\right\}}{\max\left\{d_{(x_M x_\mathtt{e} x_\mathtt{f})}^{x_K}, d_{(x_M x_\mathtt{e} x_\mathtt{f})}^{x_L}\right\}} \geq \delta,$$

and

Assumption A2 $$\frac{\min\left\{|\mathbf{n}_{x_K x_\mathtt{e}}|, |\mathbf{n}_{x_M x_\mathtt{e}}|, |\mathbf{n}_{x_L x_\mathtt{e}}|, |\mathbf{n}_{x_K x_L}|, |\mathbf{n}_{x_M x_K}|, |\mathbf{n}_{x_M x_L}|\right\}}{\max\left\{\begin{array}{l} m_{(x_M x_K x_\mathtt{e})}, m_{(x_M x_L x_\mathtt{e})}, m_{(x_K x_\mathtt{e} x_\mathtt{f})}, m_{(x_L x_\mathtt{e} x_\mathtt{f})}, \\ m_{(x_M x_\mathtt{e} x_\mathtt{f})}, \ m_{(x_M x_K x_\mathtt{f})}, \ m_{(x_M x_L x_\mathtt{f})} \end{array}\right\}} \geq \delta.$$

Then, for any $T \in \mathcal{T}_h^{**} \setminus \mathcal{T}_\Lambda^{**}$, the discrete gradient $\nabla_\Lambda \mathbf{u}_h$ is written as

$$\begin{aligned} m_T\,(\nabla_\Lambda \mathbf{u}_h)_T = {} & (u_K - u_M)(\mathbf{n}_{x_M x_K} + \boldsymbol{\epsilon}_{x_M x_K}) + (u_L - u_M)(\mathbf{n}_{x_M x_L} + \boldsymbol{\epsilon}_{x_M x_L}) \\ & + (u_\mathtt{e} - u_M)(\mathbf{n}_{x_M x_\mathtt{e}} + \boldsymbol{\epsilon}_{x_M x_\mathtt{e}}) + (u_L - u_K)(\mathbf{n}_{x_K x_L} + \boldsymbol{\epsilon}_{x_K x_L}) \\ & + (u_\mathtt{e} - u_K)(\mathbf{n}_{x_K x_\mathtt{e}} + \boldsymbol{\epsilon}_{x_K x_\mathtt{e}}) + (u_\mathtt{e} - u_L)(\mathbf{n}_{x_L x_\mathtt{e}} + \boldsymbol{\epsilon}_{x_L x_\mathtt{e}}), \end{aligned} \tag{53}$$

where the vectors $\left\{\mathbf{n}_{x_N x_Q}, \boldsymbol{\epsilon}_{x_N x_Q}\right\}_{(x_N, x_Q) \in \mathcal{V}_T^{(2)}}$ satisfy

$$\lim_{h \to 0} \frac{|\boldsymbol{\epsilon}_{x_M x_K}|}{|\mathbf{n}_{x_M x_K}|} = \lim_{h \to 0} \frac{|\boldsymbol{\epsilon}_{x_M x_L}|}{|\mathbf{n}_{x_M x_L}|} = \lim_{h \to 0} \frac{|\boldsymbol{\epsilon}_{x_M x_\mathtt{e}}|}{|\mathbf{n}_{x_M x_\mathtt{e}}|} = \lim_{h \to 0} \frac{|\boldsymbol{\epsilon}_{x_K x_L}|}{|\mathbf{n}_{x_K x_L}|}$$

$$= \lim_{h\to 0} \frac{|\boldsymbol{\epsilon}_{x_K x_e}|}{|\mathbf{n}_{x_K x_e}|} = \lim_{h\to 0} \frac{|\boldsymbol{\epsilon}_{x_L x_e}|}{|\mathbf{n}_{x_L x_e}|} = 0. \tag{54}$$

Proof In the subdual mesh, each tetrahedron $T := (x_M x_K x_L x_e) \in \mathcal{T}_h^{**} \backslash \mathcal{T}_\Lambda^{**}$ can be separated into two tetrahedrons, each including sub-tetrahedrons T_K and T_L. The tensor Λ is approximated by Λ_K and Λ_L, respectively. Thus, the discrete gradient $(\nabla_\Lambda \mathbf{u}_h)_T$, which depends on Λ_K and Λ_L, is presented in the following cases:

Case 1. If $\Lambda_K = \Lambda_L$, the discrete gradient $(\nabla_\Lambda \mathbf{u}_h)_T$ takes a form similar to (11). It is then computed as

$$\begin{aligned} m_T\,(\nabla_\Lambda \mathbf{u}_h)_T =& -(u_e - u_K)\frac{1}{4}\left[\mathbf{n}_{(x_M x_K x_L)} - \mathbf{n}_{(x_M x_L x_e)}\right] \\ & -(u_e - u_L)\frac{1}{4}\left[\mathbf{n}_{(x_M x_K x_L)} - \mathbf{n}_{(x_M x_K x_e)}\right] \\ & -(u_e - u_M)\frac{1}{4}\left[\mathbf{n}_{(x_M x_K x_L)} - \mathbf{n}_{(x_K x_L x_e)}\right] \\ & -(u_L - u_K)\frac{1}{4}\left[\mathbf{n}_{(x_M x_K x_e)} - \mathbf{n}_{(x_M x_L x_e)}\right] \\ & -(u_K - u_M)\frac{1}{4}\left[\mathbf{n}_{(x_M x_L x_e)} - \mathbf{n}_{(x_K x_L x_e)}\right] \\ & -(u_L - u_M)\frac{1}{4}\left[\mathbf{n}_{(x_M x_K x_e)} - \mathbf{n}_{(x_K x_L x_e)}\right]. \end{aligned} \tag{55}$$

Additionally, the geometrical properties of T (refer to Fig. 7) are as follows:

$$\begin{aligned} &\mathbf{n}_{x_K x_e} = -\frac{1}{4}\left[\mathbf{n}_{(x_M x_K x_L)} - \mathbf{n}_{(x_M x_L x_e)}\right], \quad \mathbf{n}_{x_M x_e} = -\frac{1}{4}\left[\mathbf{n}_{(x_M x_K x_L)} - \mathbf{n}_{(x_K x_L x_e)}\right], \\ &\mathbf{n}_{x_L x_e} = -\frac{1}{4}\left[\mathbf{n}_{(x_M x_K x_L)} - \mathbf{n}_{(x_M x_K x_e)}\right], \quad \mathbf{n}_{x_K x_L} = -\frac{1}{4}\left[\mathbf{n}_{(x_M x_K x_e)} - \mathbf{n}_{(x_M x_L x_e)}\right], \\ &\mathbf{n}_{x_M x_K} = -\frac{1}{4}\left[\mathbf{n}_{(x_M x_L x_e)} - \mathbf{n}_{(x_K x_L x_e)}\right], \quad \mathbf{n}_{x_M x_L} = -\frac{1}{4}\left[\mathbf{n}_{(x_M x_K x_e)} - \mathbf{n}_{(x_K x_L x_e)}\right]. \end{aligned} \tag{56}$$

Substituting (56) into (55), we have

$$\begin{aligned} m_T\,(\nabla_\Lambda \mathbf{u}_h)_T =& (u_e - u_K)\mathbf{n}_{x_K x_e} + (u_e - u_L)\mathbf{n}_{x_L x_e} + (u_e - u_M)\mathbf{n}_{x_M x_e} \\ & + (u_L - u_K)\mathbf{n}_{x_K x_L} + (u_K - u_M)\mathbf{n}_{x_M x_K} + (u_L - u_M)\mathbf{n}_{x_M x_L}. \end{aligned} \tag{57}$$

It is noted that the formula (57) is equivalent to (53), where all vectors $\boldsymbol{\epsilon}_{x_K x_e}$, $\boldsymbol{\epsilon}_{x_L x_e}$, $\boldsymbol{\epsilon}_{x_M x_e}$, $\boldsymbol{\epsilon}_{x_K x_L}$, $\boldsymbol{\epsilon}_{x_M x_K}$, and $\boldsymbol{\epsilon}_{x_M x_L}$ are set to $\mathbf{0}$.

Case 2. If $\Lambda_K \neq \Lambda_L$ $\left(\text{such that } \lim_{h\to 0} \|\Lambda_K - \Lambda_L\| = 0\right)$, equation (27) for the discrete gradient $(\nabla_\Lambda \mathbf{u}_h)_T$ is given as follows:

- Case 2a. On $T_K = (x_M x_K x_e x_f)$, the discrete gradient $(\nabla_\Lambda \mathbf{u}_h)_{T_K}$ is established as

$$\begin{aligned} m_{T_K}(\nabla_\Lambda \mathbf{u}_h)_{T_K} &= (u_K - u_M)(\mathbf{n}_{x_M x_K} + \boldsymbol{\epsilon}^K_{x_M x_K}) + (u_L - u_M)(\mathbf{n}_{x_M x_L} + \boldsymbol{\epsilon}^K_{x_M x_L}) \\ &+ (u_e - u_M)(\mathbf{n}_{x_M x_e} + \boldsymbol{\epsilon}^K_{x_M x_e}) + (u_L - u_K)(\mathbf{n}_{x_K x_L} + \boldsymbol{\epsilon}^K_{x_K x_L}) \\ &+ (u_e - u_K)(\mathbf{n}_{x_K x_e} + \boldsymbol{\epsilon}^K_{x_K x_e}) + (u_e - u_L)(\mathbf{n}_{x_L x_e} + \boldsymbol{\epsilon}^K_{x_L x_e}), \end{aligned} \tag{58}$$

Considering the assumptions A A1 and A A2, as $h \to 0$, the values in (17) obtain the following limits:

$$\begin{aligned} -\frac{\beta_K}{\beta_f} &\to \frac{d^{x_L}_{(x_M x_e x_f)}}{d^{x_K}_{(x_M x_e x_f)} + d^{x_L}_{(x_M x_e x_f)}}, & -\frac{\beta_M}{\beta_f} &\to 0, \\ -\frac{\beta_L}{\beta_f} &\to \frac{d^{x_K}_{(x_M x_e x_f)}}{d^{x_K}_{(x_M x_e x_f)} + d^{x_L}_{(x_M x_e x_f)}}, & -\frac{\beta_e}{\beta_f} &\to 0. \end{aligned}$$

The vectors in (58) satisfy the following convergences:

$$\begin{aligned} \frac{|\boldsymbol{\epsilon}^K_{x_K x_e}|}{|\mathbf{n}_{x_K x_e}|} &= \left| \left(-\frac{m_{[x_K x_L]}}{m_{[x_K x_f]}} \frac{\beta_e}{\beta_f} - 1 + \frac{m_T}{m_{T_K}} + \frac{m_T}{m_{T_K}} \frac{\beta_K}{\beta_f} \right) \right| \frac{3m_{(x_M x_K x_e)}}{m_{(x_M x_L C_{[x_K x_e]})}} \to 0, \\ \frac{|\boldsymbol{\epsilon}^K_{x_L x_e}|}{|\mathbf{n}_{x_L x_e}|} &= \left| \left(-\frac{m_{[x_K x_L]}}{m_{[x_K x_f]}} \frac{\beta_e}{\beta_f} + 1 + \frac{m_T}{m_{T_K}} \frac{\beta_L}{\beta_f} \right) \right| \frac{3m_{(x_M x_K x_e)}}{m_{(x_M x_K C_{[x_L x_e]})}} \to 0, \\ \frac{|\boldsymbol{\epsilon}^K_{x_M x_e}|}{|\mathbf{n}_{x_M x_e}|} &= \left| \frac{m_{[x_K x_L]}}{m_{[x_K x_f]}} \left(-\frac{\beta_e}{\beta_f} + \frac{\beta_M}{\beta_f} \right) \right| \frac{3m_{(x_M x_K x_e)}}{m_{(x_K x_L C_{[x_M x_e]})}} \to 0, \\ \frac{|\boldsymbol{\epsilon}^K_{x_K x_L}|}{|\mathbf{n}_{x_K x_L}|} &= \left| \left(-1 - \frac{m_T}{m_{T_K}} \frac{\beta_L}{\beta_f} - 1 + \frac{m_T}{m_{T_K}} + \frac{m_T}{m_{T_K}} \frac{\beta_K}{\beta_f} \right) \right| \frac{3m_{(x_M x_K x_e)}}{m_{(x_M x_e C_{[x_K x_L]})}} \to 0, \\ \frac{|\boldsymbol{\epsilon}^K_{x_M x_K}|}{|\mathbf{n}_{x_M x_K}|} &= \left| \left(1 - \frac{m_T}{m_{T_K}} - \frac{m_T}{m_{T_K}} \frac{\beta_K}{\beta_f} + \frac{m_{[x_K x_L]}}{m_{[x_K x_f]}} \frac{\beta_M}{\beta_f} \right) \right| \frac{3m_{(x_M x_K x_e)}}{m_{(x_L x_e C_{[x_M x_K]})}} \to 0, \\ \frac{|\boldsymbol{\epsilon}^K_{x_M x_L}|}{|\mathbf{n}_{x_M x_L}|} &= \left| \left(-1 - \frac{m_T}{m_{T_K}} \frac{\beta_L}{\beta_f} + \frac{m_{[x_K x_L]}}{m_{[x_K x_f]}} \frac{\beta_M}{\beta_f} \right) \right| \frac{3m_{(x_M x_K x_e)}}{m_{(x_K x_e C_{[x_M x_L]})}} \to 0, \end{aligned} \tag{59}$$

as $h \to 0$.

- Case 2b. On $T_L = (x_M x_L x_e x_f)$, the results can be computed as in Case 2a, specifically as follows:

$$\begin{aligned} m_{T_L}(\nabla_\Lambda \mathbf{u}_h)_{T_L} &= (u_K - u_M)(\mathbf{n}_{x_M x_K} + \boldsymbol{\epsilon}^L_{x_M x_K}) + (u_L - u_M)(\mathbf{n}_{x_M x_L} + \boldsymbol{\epsilon}^L_{x_M x_L}) \\ &+ (u_e - u_M)(\mathbf{n}_{x_M x_e} + \boldsymbol{\epsilon}^K_{x_M x_e}) + (u_L - u_K)(\mathbf{n}_{x_K x_L} + \boldsymbol{\epsilon}^L_{x_K x_L}) \\ &+ (u_e - u_K)(\mathbf{n}_{x_K x_e} + \boldsymbol{\epsilon}^L_{x_K x_e}) + (u_e - u_L)(\mathbf{n}_{x_L x_e} + \boldsymbol{\epsilon}^L_{x_L x_e}), \end{aligned} \tag{60}$$

whose vectors satisfy

$$\frac{|\boldsymbol{\epsilon}^{L}_{x_N x_Q}|}{|\mathbf{n}_{x_N x_Q}|} \to 0, \quad \forall (x_N, x_Q) \in \mathcal{V}_T^{(2)}, \quad h \to 0. \tag{61}$$

From (58)–(61), we obtain the formula $(\nabla_\Lambda \mathbf{u}_h)_T$ as given in (53), where the vectors $\boldsymbol{\epsilon}_{x_N x_Q}$ are determined by $\boldsymbol{\epsilon}^{K}_{x_N x_Q}$ and $\boldsymbol{\epsilon}^{L}_{x_N x_Q}$ on T_K and T_L, respectively, for all $(x_N, x_Q) \in \mathcal{V}_T^{(2)}$.

If $T := (x_M x_K x_{\mathrm{e}} x_{\mathrm{f}}) \in \mathcal{T}^{**}_{\mathrm{const}}$, the tensor Λ has only one approximation Λ_K on T, then $(\nabla_\Lambda \mathbf{u}_h)_T$ is expressed as in (57):

$$\begin{aligned} m_T\,(\nabla_\Lambda \mathbf{u}_h)_T = {} & (u_{\mathrm{e}} - u_K)\mathbf{n}_{x_K x_{\mathrm{e}}} + (u_{\mathrm{e}} - u^M_{\mathrm{f}})\mathbf{n}_{x_L x_{\mathrm{e}}} + (u_{\mathrm{e}} - u_M)\mathbf{n}_{x_M x_{\mathrm{e}}} \\ & + (u^M_{\mathrm{f}} - u_K)\mathbf{n}_{x_K x_{\mathrm{f}}} + (u_K - u_M)\mathbf{n}_{x_M x_K} + (u^M_{\mathrm{f}} - u_M)\mathbf{n}_{x_M x_{\mathrm{f}}}. \end{aligned} \tag{62}$$

□

Lemma 2 *Let $(\mathcal{H}_h, h, P_1, \nabla_\Lambda)$ be a family of discretizations in the sense of Definition 2 and let δ be a positive constant independent of h such that*

Assumption A3

$$\begin{aligned} & \left| \frac{\left(\Lambda_K \mathbf{n}_{(x_M x_K x_{\mathrm{e}})}\right) \cdot \mathbf{n}^K_{(x_M x_{\mathrm{e}} x_{\mathrm{f}})}}{m_{T_K}} - \frac{\left(\Lambda_L \mathbf{n}_{(x_M x_L x_{\mathrm{e}})}\right) \cdot \mathbf{n}^K_{(x_M x_{\mathrm{e}} x_{\mathrm{f}})}}{m_{T_L}} \right| \\ & \geq \delta \max \left\{ \frac{\left(\Lambda_K \mathbf{n}^K_{(x_M x_{\mathrm{e}} x_{\mathrm{f}})}\right) \cdot \mathbf{n}^K_{(x_M x_{\mathrm{e}} x_{\mathrm{f}})}}{m_{T_K}} + \frac{\left(\Lambda_L \mathbf{n}^K_{(x_M x_{\mathrm{e}} x_{\mathrm{f}})}\right) \cdot \mathbf{n}^K_{(x_M x_{\mathrm{e}} x_{\mathrm{f}})}}{m_{T_L}}, \right. \\ & \qquad \left. \left| \frac{\left(\Lambda_K \mathbf{n}_{(x_M x_K x_{\mathrm{f}})}\right) \cdot \mathbf{n}^K_{(x_M x_{\mathrm{e}} x_{\mathrm{f}})}}{m_{T_K}} - \frac{\left(\Lambda_L \mathbf{n}_{(x_M x_L x_{\mathrm{f}})}\right) \cdot \mathbf{n}^K_{(x_M x_{\mathrm{e}} x_{\mathrm{f}})}}{m_{T_L}} \right| \right\}, \end{aligned} \tag{63}$$

for any $T := (x_M x_K x_L x_{\mathrm{e}}) \in \mathcal{T}^{**}_\Lambda$.

On each sub-tetrahedron T_K and T_L of T, the discrete gradient $\nabla_\Lambda \mathbf{u}_h$ is rewritten as

$$\begin{aligned} |T_K|(\nabla_\Lambda \mathbf{u}_h)_{T_K} = {} & (u_K - u_M)\boldsymbol{\tau}^{T_K}_{x_M x_K} + (u_L - u_M)\boldsymbol{\tau}^{T_K}_{x_M x_L} + (u_{\mathrm{e}} - u_M)\boldsymbol{\tau}^{T_K}_{x_M x_{\mathrm{e}}} \\ & + (u_L - u_K)\boldsymbol{\tau}^{T_K}_{x_K x_L} + (u_{\mathrm{e}} - u_K)\boldsymbol{\tau}^{T_K}_{x_K x_{\mathrm{e}}} + (u_{\mathrm{e}} - u_L)\boldsymbol{\tau}^{T_K}_{x_L x_{\mathrm{e}}}, \end{aligned} \tag{64}$$

$$\begin{aligned} |T_L|(\nabla_\Lambda \mathbf{u}_h)_{T_L} = {} & (u_K - u_M)\boldsymbol{\tau}^{T_L}_{x_M x_K} + (u_L - u_M)\boldsymbol{\tau}^{T_L}_{x_M x_L} + (u_{\mathrm{e}} - u_M)\boldsymbol{\tau}^{T_L}_{x_M x_{\mathrm{e}}} \\ & + (u_L - u_K)\boldsymbol{\tau}^{T_L}_{x_K x_L} + (u_{\mathrm{e}} - u_K)\boldsymbol{\tau}^{T_L}_{x_K x_{\mathrm{e}}} + (u_{\mathrm{e}} - u_L)\boldsymbol{\tau}^{T_L}_{x_L x_{\mathrm{e}}}, \end{aligned} \tag{65}$$

respectively, and

$$|\boldsymbol{\tau}^{T_K}_{x_N x_Q}|, \ |\boldsymbol{\tau}^{T_L}_{x_N x_Q}| \leq C_1 |\mathbf{n}_{x_N x_Q}|, \quad (x_N, x_Q) \in \mathcal{V}_T^{(2)}, \tag{66}$$

where the positive constant C_1 depends on δ.

Proof Substituting (20) into the first equation in (27) yields

$$(\nabla_\Lambda \mathbf{u}_h)_{T_K} = -\frac{\left[\begin{array}{l}(u_{\mathrm{e}} - u_K)\,\boldsymbol{\tau}_{x_K x_{\mathrm{e}}}^{T_K} + (u_{\mathrm{e}} - u_L)\,\boldsymbol{\tau}_{x_L x_{\mathrm{e}}}^{T_K} + (u_{\mathrm{e}} - u_M)\,\boldsymbol{\tau}_{x_M x_{\mathrm{e}}}^{T_K} + \\ (u_L - u_K)\,\boldsymbol{\tau}_{x_K x_L}^{T_K} + (u_K - u_M)\,\boldsymbol{\tau}_{x_M x_K}^{T_K} + (u_L - u_M)\,\boldsymbol{\tau}_{x_M x_L}^{T_K}\end{array}\right]}{3m_{T_K}}, \tag{67}$$

with

$$\begin{aligned}
\boldsymbol{\tau}_{x_M x_K}^{T_K} &= \left(\widetilde{\beta}_M^T \mathbf{n}_{(x_M x_{\mathrm{e}} x_{\mathrm{f}})}^K - \widetilde{\beta}_K^T \mathbf{n}_{(x_K x_{\mathrm{e}} x_{\mathrm{f}})}\right), \qquad \boldsymbol{\tau}_{x_K x_L}^{T_K} = \left(-\widetilde{\beta}_L^T \mathbf{n}_{(x_M x_{\mathrm{e}} x_{\mathrm{f}})}^K\right),\\
\boldsymbol{\tau}_{x_M x_{\mathrm{e}}}^{T_K} &= \left(-\mathbf{n}_{(x_K x_{\mathrm{e}} x_{\mathrm{f}})} + \widetilde{\beta}_M^T \mathbf{n}_{(x_M x_K x_{\mathrm{f}})}\right), \qquad \boldsymbol{\tau}_{x_M x_L}^{T_K} = \left(-\widetilde{\beta}_L^T \mathbf{n}_{(x_K x_{\mathrm{e}} x_{\mathrm{f}})}\right),\\
\boldsymbol{\tau}_{x_K x_{\mathrm{e}}}^{T_K} &= \left(\widetilde{\beta}_K^T \mathbf{n}_{(x_M x_K x_{\mathrm{f}})} - \widetilde{\beta}_e^T \mathbf{n}_{(x_M x_{\mathrm{e}} x_{\mathrm{f}})}^K\right), \qquad \boldsymbol{\tau}_{x_L x_{\mathrm{e}}}^{T_K} = \left(\widetilde{\beta}_L^T \mathbf{n}_{(x_M x_K x_{\mathrm{f}})}\right).
\end{aligned} \tag{68}$$

Regarding assumptions A A2 and A A3, the inequalities between the magnitudes of the aforementioned vectors and $\left\{|\mathbf{n}_{x_N x_Q}|\right\}_{(x_N, x_Q)\in\mathcal{V}_T^{(2)}}$ are as follows:

$$\begin{aligned}
&\left|\boldsymbol{\tau}_{x_M x_K}^{T_K}\right| \le \max\left\{|\widetilde{\beta}_M^T|,\ |\widetilde{\beta}_K^T|\right\}\left(|\mathbf{n}_{(x_M x_{\mathrm{e}} x_{\mathrm{f}})}^K| + |\mathbf{n}_{(x_K x_{\mathrm{e}} x_{\mathrm{f}})}|\right) \le \frac{\delta+3}{\delta^2}|\mathbf{n}_{x_M x_K}|,\\
&\left|\boldsymbol{\tau}_{x_M x_L}^{T_K}\right| \le \frac{1}{\delta^2}|\mathbf{n}_{x_M x_L}|,\\
&\left|\boldsymbol{\tau}_{x_M x_{\mathrm{e}}}^{T_K}\right| \le \max\left\{1, \left|\widetilde{\beta}_M^T\right|\right\}\left(|\mathbf{n}_{(x_K x_{\mathrm{e}} x_{\mathrm{f}})}| + |\mathbf{n}_{(x_M x_K x_{\mathrm{f}})}|\right) \le \frac{2(\delta+3)}{\delta^2}|\mathbf{n}_{x_M x_{\mathrm{e}}}|,\\
&\left|\boldsymbol{\tau}_{x_K x_L}^{T_K}\right| \le \frac{1}{\delta^2}|\mathbf{n}_{x_K x_L}|,\\
&\left|\boldsymbol{\tau}_{x_K x_{\mathrm{e}}}^{T_K}\right| \le \max\left\{\left|\widetilde{\beta}_K^T\right|,\ \left|\widetilde{\beta}_e^T\right|\right\}\left(|\mathbf{n}_{(x_M x_K x_{\mathrm{f}})}| + |\mathbf{n}_{(x_M x_{\mathrm{e}} x_{\mathrm{f}})}^K|\right) \le \frac{2}{\delta^2}|\mathbf{n}_{x_K x_{\mathrm{e}}}|,\\
&\left|\boldsymbol{\tau}_{x_L x_{\mathrm{e}}}^{T_K}\right| \le \frac{1}{\delta^2}|\mathbf{n}_{x_L x_{\mathrm{e}}}|,
\end{aligned}$$

where the coefficients $\widetilde{\beta}_M^T$, $\widetilde{\beta}_K^T$, $\widetilde{\beta}_L^T$, and $\widetilde{\beta}_e^T$ are given in (19) and satisfy the following upper bounds:

$$\begin{aligned}
&\left|\widetilde{\beta}_M^T\right| \le 1 + |\widetilde{\beta}_K^T| + |\widetilde{\beta}_L^T| + |\widetilde{\beta}_e^T| \le 1 + \frac{3}{\delta},\\
&\left|\widetilde{\beta}_K^T\right| = \left|\frac{\left(\Lambda_K \mathbf{n}_{(x_M x_{\mathrm{e}} x_{\mathrm{f}})}^K\right)\cdot \mathbf{n}_{(x_M x_{\mathrm{e}} x_{\mathrm{f}})}^K}{3m_{T_K}\beta_{\mathrm{f}}}\right| \le \frac{1}{\delta},\\
&\left|\widetilde{\beta}_e^T\right| = \left|\frac{\left(\Lambda_K \mathbf{n}_{(x_M x_K x_{\mathrm{f}})}\right)\cdot \mathbf{n}_{(x_M x_{\mathrm{e}} x_{\mathrm{f}})}^K}{3m_{T_K}\beta_{\mathrm{f}}} - \frac{\left(\Lambda_L \mathbf{n}_{(x_M x_L x_{\mathrm{f}})}\right)\cdot \mathbf{n}_{(x_M x_{\mathrm{e}} x_{\mathrm{f}})}^K}{3m_{T_L}\beta_{\mathrm{f}}}\right| \le \frac{1}{\delta},
\end{aligned}$$

$$\left|\widetilde{\beta}_L^T\right| = \left|\frac{\left(\Lambda_L \mathbf{n}^L_{(x_M x_e x_f)}\right)\cdot \mathbf{n}^L_{(x_M x_e x_f)}}{3m_{T_L}\beta_f}\right| \le \frac{1}{\delta}.$$

In this expression, the coefficient $C_1 = \frac{2(\delta+3)}{\delta^2}$ satisfies (66). □

Proposition 2 *Under the assumptions A A1–A A3, let $(\mathcal{H}_h, h, P_1, \nabla_\Lambda)$ be a family of discretizations in the sense of Definition 2. A positive constant δ independent of h satisfies the following conditions:*

Assumption A4 $\frac{d_{x_K x_e}}{m_{[x_K x_e]}}, \frac{d_{x_L x_e}}{m_{[x_L x_e]}}, \frac{d_{x_M x_e}}{m_{[x_M x_e]}}, \frac{d_{x_K x_L}}{m_{[x_K x_L]}}, \frac{d_{x_K x_M}}{m_{[x_K x_M]}}, \frac{d_{x_L x_M}}{m_{[x_L x_M]}} \ge \delta,$

Assumption A5
$$\frac{\min\limits_{Q\in\{K,L\}}\left\{\begin{matrix} m_{f^{T_Q}_{(x_M x_K C_{[x_L x_e]})}}, m_{f^{T_Q}_{(x_M x_L C_{[x_K x_e]})}}, m_{f^{T_Q}_{(x_K x_L C_{[x_M x_e]})}}, \\ m_{f^{T_Q}_{(x_K x_e C_{[x_M x_L]})}}, m_{f^{T_Q}_{(x_L x_e C_{[x_M x_K]})}} \end{matrix}\right\}}{\max\left\{\begin{matrix} m_{(x_M x_K C_{[x_L x_e]})}, m_{(x_M x_L C_{[x_K x_e]})}, m_{(x_K x_L C_{[x_M x_e]})}, \\ m_{(x_K x_e C_{[x_M x_L]})}, m_{(x_L x_e C_{[x_M x_K]})} \end{matrix}\right\}} \ge \delta,$$

where the planar parts $f^{T_Q}_{(x_M x_K C_{[x_L x_e]})}$, $f^{T_Q}_{(x_M x_L C_{[x_K x_e]})}$, $f^{T_Q}_{(x_K x_L C_{[x_M x_e]})}$, $f^{T_Q}_{(x_K x_e C_{[x_M x_L]})}$ and $f^{T_Q}_{(x_L x_e C_{[x_M x_K]})}$ of the respective faces $(x_M x_K C_{[x_L x_e]})$, $(x_M x_L C_{[x_K x_e]})$, $(x_K x_L C_{[x_M x_e]})$, $(x_K x_e C_{[x_M x_L]})$, and $(x_L x_e C_{[x_M x_K]})$ are within the tetrahedron T_Q for each $Q \in \{K, L\}$.

Assumption A6 $\frac{\rho_{T_K}}{h_T}, \frac{\rho_{T_L}}{h_T} \ge \delta,$

Then, the EFC-3DFEMb scheme is coercive, meaning that there exists a positive constant C_2 independent of h such that

$$\|P_1 \mathbf{v}_h\|_{L^2(\Omega)} \le C_2 \|\nabla_\Lambda \mathbf{v}_h\|_{(L^2(\Omega))^2}, \quad \forall \mathbf{v}_h \in \mathcal{H}_h. \tag{69}$$

The EFC-3DFEMb scheme also satisfies the following limits:

$$\lim_{h\to 0} \widehat{S}_h(\varphi) = 0, \quad \forall \varphi \in C_c^\infty(\Omega), \tag{70}$$

$$\lim_{h\to 0} \widehat{W}_h(\boldsymbol{\varphi}) = 0, \quad \forall \boldsymbol{\varphi} \in \left(C_c^\infty(\Omega)\right)^3, \tag{71}$$

where the operators $\widehat{S}_h$ and $\widehat{W}_h$ are defined by (49) and (50), respectively.

Proof We verify the existence of a positive constant C_3 depending on Ω and δ such that

$$\|\mathbf{v}_h\|^2_{1,\mathcal{T}_h^{**}} \le C_3 \|\nabla_\Lambda \mathbf{v}_h\|^2_{(L^2(\Omega))^2}, \quad \forall \mathbf{v}_h \in \mathcal{H}_h, \tag{72}$$

as follows: For any tetrahedron $T := (x_M x_K x_L x_e) \in \mathcal{T}_h^{**}$, the formula for $\nabla_\Lambda \mathbf{v}_h$ in classifying T can be obtained by

Case 1: If $T \in \mathcal{T}^{**}_{\text{const}}$, $(\nabla_\Lambda \mathbf{v}_h)_T$ is then calculated as given in (57). This equation satisfies

$$\begin{aligned}
v_\mathrm{e} - v_K &= (\nabla_\Lambda \mathbf{v}_h)_T \cdot (x_\mathrm{e} - x_K), & v_\mathrm{e} - v_L &= (\nabla_\Lambda \mathbf{v}_h)_T \cdot (x_\mathrm{e} - x_L),\\
v_\mathrm{e} - v_M &= (\nabla_\Lambda \mathbf{v}_h)_T \cdot (x_\mathrm{e} - x_M), & v_L - v_K &= (\nabla_\Lambda \mathbf{v}_h)_T \cdot (x_L - x_K),\\
v_K - v_M &= (\nabla_\Lambda \mathbf{v}_h)_T \cdot (x_K - x_M), & v_L - v_M &= (\nabla_\Lambda \mathbf{v}_h)_T \cdot (x_L - x_M),
\end{aligned}$$

Therefore,

$$\begin{aligned}
\|(\nabla_\Lambda \mathbf{v}_h)_T\|^2 &\geq \frac{|v_\mathrm{e} - v_K|^2}{m^2_{[x_K x_\mathrm{e}]}}, & \|(\nabla_\Lambda \mathbf{v}_h)_T\|^2 &\geq \frac{|v_\mathrm{e} - v_L|^2}{m^2_{[x_L x_\mathrm{e}]}},\\
\|(\nabla_\Lambda \mathbf{v}_h)_T\|^2 &\geq \frac{|v_\mathrm{e} - v_M|^2}{m^2_{[x_M x_\mathrm{e}]}}, & \|(\nabla_\Lambda \mathbf{v}_h)_T\|^2 &\geq \frac{|v_L - v_K|^2}{m^2_{[x_K x_L]}},\\
\|(\nabla_\Lambda \mathbf{v}_h)_T\|^2 &\geq \frac{|v_M - v_K|^2}{m^2_{[x_K x_M]}}, & \|(\nabla_\Lambda \mathbf{v}_h)_T\|^2 &\geq \frac{|v_L - v_M|^2}{m^2_{[x_L x_M]}}.
\end{aligned} \tag{73}$$

Additionally, $\frac{m_T}{m^2_{[x_K x_\mathrm{e}]}} \geq \frac{\delta^2}{3}\frac{|\mathbf{n}_{x_K x_\mathrm{e}}|}{d_{x_K x_\mathrm{e}}}$ from $m_T \geq m_{(x_K, x_\mathrm{e}, \mathfrak{f}_{[x_K x_\mathrm{e}]})} = \frac{1}{3} d_{x_K x_\mathrm{e}} |\mathbf{n}_{x_K x_\mathrm{e}}|$ and $d_{x_K x_\mathrm{e}} \leq m_{[x_K x_\mathrm{e}]}$. In the same manner, it has

$$\begin{aligned}
&\frac{m_T}{m^2_{[x_L x_\mathrm{e}]}} \geq \frac{\delta^2}{3}\frac{|\mathbf{n}_{x_L x_\mathrm{e}}|}{d_{x_L x_\mathrm{e}}}, \quad \frac{m_T}{m^2_{[x_M x_\mathrm{e}]}} \geq \frac{\delta^2}{3}\frac{|\mathbf{n}_{x_M x_\mathrm{e}}|}{d_{x_M x_\mathrm{e}}}, \quad \frac{m_T}{m^2_{[x_K x_L]}} \geq \frac{\delta^2}{3}\frac{|\mathbf{n}_{x_K x_L}|}{d_{x_K x_L}},\\
&\frac{m_T}{m^2_{[x_K x_M]}} \geq \frac{\delta^2}{3}\frac{|\mathbf{n}_{x_K x_M}|}{d_{x_K x_M}}, \quad \frac{m_T}{m^2_{[x_L x_M]}} \geq \frac{\delta^2}{3}\frac{|\mathbf{n}_{x_L x_M}|}{d_{x_L x_M}}, \quad \frac{m_T}{m^2_{[x_K x_\mathrm{e}]}} \geq \frac{\delta^2}{3}\frac{|\mathbf{n}_{x_K x_\mathrm{e}}|}{d_{x_K x_\mathrm{e}}}.
\end{aligned} \tag{74}$$

From Eqs. (73) and (74), it follows that

$$\begin{aligned}
m_T \|(\nabla_\Lambda \mathbf{v}_h)_T\|^2 &\geq \frac{1}{6} m_T \begin{bmatrix} \frac{|v_\mathrm{e} - v_K|^2}{m^2_{[x_K x_\mathrm{e}]}} + \frac{|v_\mathrm{e} - v_L|^2}{m^2_{[x_L x_\mathrm{e}]}} + \frac{|v_\mathrm{e} - v_M|^2}{m^2_{[x_M x_\mathrm{e}]}} + \\ \frac{|v_L - v_K|^2}{m^2_{[x_K x_L]}} + \frac{|v_M - v_K|^2}{m^2_{[x_K x_M]}} + \frac{|v_L - v_M|^2}{m^2_{[x_L x_M]}} \end{bmatrix}\\
&\geq \frac{\delta^2}{18} \begin{bmatrix} \frac{|\mathbf{n}_{x_K x_\mathrm{e}}|}{d_{x_K x_\mathrm{e}}}(v_e - v_K)^2 + \frac{|\mathbf{n}_{x_L x_\mathrm{e}}|}{d_{x_L x_\mathrm{e}}}(v_e - v_L)^2 + \frac{|\mathbf{n}_{x_M x_\mathrm{e}}|}{d_{x_M x_\mathrm{e}}}(v_e - v_M)^2 + \\ \frac{|\mathbf{n}_{x_K x_L}|}{d_{x_K x_L}}(v_L - v_K)^2 + \frac{|\mathbf{n}_{x_M x_K}|}{d_{x_M x_K}}(v_K - v_M)^2 + \frac{|\mathbf{n}_{x_M x_L}|}{d_{x_M x_L}}(v_L - v_M)^2 \end{bmatrix}.
\end{aligned} \tag{75}$$

Case 2: If $T \in \mathcal{T}^{**}_h \setminus \mathcal{T}^{**}_{\text{const}}$, $\nabla_\Lambda \mathbf{u}_h$ is defined by (27). Considering $\nabla_\Lambda \mathbf{v}_h$ on T_K, it has

$$\begin{aligned}
v_\mathrm{e} - v_K &= (\nabla_\Lambda \mathbf{v}_h)_{T_K} \cdot (x_\mathrm{e} - x_K), & v_\mathrm{e} - v^M_\mathfrak{f} &= (\nabla_\Lambda \mathbf{v}_h)_{T_K} \cdot (x_\mathrm{e} - x_\mathfrak{f}),\\
v_\mathrm{e} - v_M &= (\nabla_\Lambda \mathbf{v}_h)_{T_K} \cdot (x_\mathrm{e} - x_M), & v^M_\mathfrak{f} - v_K &= (\nabla_\Lambda \mathbf{v}_h)_{T_K} \cdot (x_\mathfrak{f} - x_K),
\end{aligned}$$

$$v_K - v_M = (\nabla_\Lambda \mathbf{v}_h)_{T_K} \cdot (x_K - x_M), \quad v_{\mathfrak{f}}^M - v_M = (\nabla_\Lambda \mathbf{v}_h)_{T_K} \cdot (x_{\mathfrak{f}} - x_M),$$

Therefore,

$$\begin{aligned}
\|(\nabla_\Lambda \mathbf{v}_h)_{T_K}\|^2 &\geq \frac{|v_{\mathfrak{e}} - v_K|^2}{m^2_{[x_K x_{\mathfrak{e}}]}}, \qquad \|(\nabla_\Lambda \mathbf{v}_h)_{T_K}\|^2 \geq \frac{\left|v_{\mathfrak{e}} - v_{\mathfrak{f}}^M\right|^2}{m^2_{[x_{\mathfrak{f}} x_{\mathfrak{e}}]}}, \\
\|(\nabla_\Lambda \mathbf{v}_h)_{T_K}\|^2 &\geq \frac{|v_{\mathfrak{e}} - v_M|^2}{m^2_{[x_M x_{\mathfrak{e}}]}}, \qquad \|(\nabla_\Lambda \mathbf{v}_h)_{T_K}\|^2 \geq \frac{\left|v_{\mathfrak{f}}^M - v_K\right|^2}{m^2_{[x_K x_{\mathfrak{f}}]}}, \qquad (76) \\
\|(\nabla_\Lambda \mathbf{v}_h)_{T_K}\|^2 &\geq \frac{|v_M - v_K|^2}{m^2_{[x_K x_M]}}, \qquad \|(\nabla_\Lambda \mathbf{v}_h)_{T_K}\|^2 \geq \frac{\left|v_{\mathfrak{f}}^M - v_M\right|^2}{m^2_{[x_M x_{\mathfrak{f}}]}}. \qquad (77)
\end{aligned}$$

Then, the inequality is established as

$$m_{T_K}\|(\nabla_\Lambda \mathbf{v}_h)_{T_K}\|^2 \geq \frac{1}{6} m_{T_K} \begin{bmatrix} \frac{|v_{\mathfrak{e}} - v_K|^2}{m^2_{[x_K x_{\mathfrak{e}}]}} + \frac{\left|v_{\mathfrak{e}} - v_{\mathfrak{f}}^M\right|^2}{m^2_{[x_{\mathfrak{e}} x_{\mathfrak{f}}]}} + \frac{|v_{\mathfrak{e}} - v_M|^2}{m^2_{[x_M x_{\mathfrak{e}}]}} + \\ \frac{\left|v_{\mathfrak{f}}^M - v_K\right|^2}{m^2_{[x_K x_{\mathfrak{f}}]}} + \frac{|v_M - v_K|^2}{m^2_{[x_K x_M]}} + \frac{\left|v_{\mathfrak{f}}^M - v_M\right|^2}{m^2_{[x_M x_{\mathfrak{f}}]}} \end{bmatrix}. \qquad (78)$$

In the same manner, the inequality on the tetrahedron T_L can be obtained as

$$m_{T_L}\|(\nabla_\Lambda \mathbf{v}_h)_{T_L}\|^2 \geq \frac{1}{6} m_{T_L} \begin{bmatrix} \frac{|v_{\mathfrak{e}} - v_L|^2}{m^2_{[x_L x_{\mathfrak{e}}]}} + \frac{\left|v_{\mathfrak{e}} - v_{\mathfrak{f}}^M\right|^2}{m^2_{[x_{\mathfrak{e}} x_{\mathfrak{f}}]}} + \frac{|v_{\mathfrak{e}} - v_M|^2}{m^2_{[x_M x_{\mathfrak{e}}]}} + \\ \frac{\left|v_{\mathfrak{f}}^M - v_L\right|^2}{m^2_{[x_L x_{\mathfrak{f}}]}} + \frac{|v_M - v_L|^2}{m^2_{[x_L x_M]}} + \frac{\left|v_{\mathfrak{f}}^M - v_M\right|^2}{m^2_{[x_M x_{\mathfrak{f}}]}} \end{bmatrix}. \qquad (79)$$

Besides, by the assumptions A A4-A A6, it holds that

$$\begin{aligned}
&\frac{m_T}{m^2_{[x_K x_{\mathfrak{e}}]}} \geq \frac{d_{x_K x_{\mathfrak{e}}} |\mathbf{n}_{x_K x_{\mathfrak{e}}}|}{3 m^2_{[x_K x_{\mathfrak{e}}]}} \geq \frac{\delta^2}{3} \frac{|\mathbf{n}_{x_K x_{\mathfrak{e}}}|}{d_{x_K x_{\mathfrak{e}}}}, \\
&\frac{m_{T_K}}{m^2_{[x_M x_K]}} \geq \frac{d_{x_M x_K} m_{\mathfrak{f}^{T_K}_{(x_L x_{\mathfrak{e}} C_{[x_M x_K]})}}}{3 m^2_{[x_M x_K]}} \geq \delta^3 \frac{|\mathbf{n}_{[x_M x_K]}|}{d_{[x_M x_K]}}, \\
&\frac{m_{T_L}}{m^2_{[x_L x_{\mathfrak{e}}]}} \geq \frac{1}{3} \frac{d_{x_L x_{\mathfrak{e}}} m_{\mathfrak{f}^{T_L}_{(x_M x_K C_{[x_L x_{\mathfrak{e}}]})}}}{m^2_{[x_L x_{\mathfrak{e}}]}} \geq \delta^3 \frac{|\mathbf{n}_{[x_L x_{\mathfrak{e}}]}|}{d_{[x_L x_{\mathfrak{e}}]}}, \\
&\frac{m_{T_L}}{m^2_{[x_M x_L]}} \geq \frac{1}{3} \frac{d_{x_M x_L} m_{\mathfrak{f}^{T_L}_{(x_K x_{\mathfrak{e}} C_{[x_M x_L]})}}}{m^2_{[x_L x_{\mathfrak{e}}]}} \geq \delta^3 \frac{|\mathbf{n}_{[x_M x_L]}|}{d_{[x_M x_L]}}, \\
&\frac{\min\left\{m_{T_K}, m_{T_L}\right\}}{m^2_{[x_K x_L]}} \geq \delta \frac{d_{x_K x_L} m_{\mathfrak{f}_{[x_K x_L]}}}{m^2_{[x_K x_L]}} \geq \delta^3 \frac{|\mathbf{n}_{[x_K x_L]}|}{d_{[x_K x_L]}}, \\
&\frac{m_T}{m^2_{[x_M x_{\mathfrak{e}}]}} \geq \frac{1}{3} \frac{d_{x_M x_{\mathfrak{e}}} m_{\mathfrak{f}_{[x_M x_{\mathfrak{e}}]}}}{m^2_{[x_M x_{\mathfrak{e}}]}} \geq \delta \frac{|\mathbf{n}_{[x_M x_{\mathfrak{e}}]}|}{d_{x_M x_{\mathfrak{e}}}},
\end{aligned}$$

$$\frac{m_{T_K}}{m^2_{[x_K x_\mathrm{f}]}} \geq \frac{m_{T_K}}{m^2_{[x_K x_L]}}, \quad \frac{m_{T_L}}{m^2_{[x_L x_\mathrm{f}]}} \geq \frac{m_{T_L}}{m^2_{[x_K x_L]}},$$
$$\text{because of } m_{[x_K x_L]} \geq m_{[x_K x_\mathrm{f}]},\ m_{[x_L x_\mathrm{f}]}. \tag{80}$$

Substituting (80) into the inequalities (78) and (79) yields:

$$\begin{aligned}
&6m_T \| (\nabla_\Lambda \mathbf{v}_h)_T \|^2 \\
&\geq \begin{bmatrix}
\frac{m_{T_K}}{m^2_{[x_K x_\mathrm{e}]}} (v_\mathrm{e} - v_K)^2 + \frac{m_{T_L}}{m^2_{[x_L x_\mathrm{e}]}} (v_\mathrm{e} - v_L)^2 + \frac{m_{T_K}}{m^2_{[x_M x_K]}} (v_K - v_M)^2 + \\
\frac{m_T}{m^2_{[x_M x_\mathrm{e}]}} (v_\mathrm{e} - v_M)^2 + \frac{m_{T_L}}{m^2_{[x_M x_L]}} (v_L - v_M)^2 + \\
\frac{m_{T_K}}{m^2_{[x_K x_\mathrm{f}]}} \left(v^M_\mathrm{f} - v_K\right)^2 + \frac{m_{T_L}}{m^2_{[x_L x_\mathrm{f}]}} \left(v^M_\mathrm{f} - v_L\right)^2 + \\
\frac{m_T}{m^2_{[x_M x_\mathrm{f}]}} \left(v^M_\mathrm{f} - v_M\right)^2 + \frac{m_T}{m^2_{[x_\mathrm{e} x_\mathrm{f}]}} \left(v^M_\mathrm{f} - v_\mathrm{e}\right)^2
\end{bmatrix} \\
&\geq \min\left\{\frac{\delta^3}{2},\ \delta\left(1 + \frac{1}{2\delta}\right)\right\} \\
&\begin{bmatrix}
\frac{|\mathbf{n}_{[x_K x_\mathrm{e}]}|}{d_{[x_K x_\mathrm{e}]}} (v_\mathrm{e} - v_K)^2 + \frac{|\mathbf{n}_{[x_L x_\mathrm{e}]}|}{d_{[x_L x_\mathrm{e}]}} (v_\mathrm{e} - v_L)^2 + \frac{|\mathbf{n}_{[x_M x_K]}|}{d_{[x_M x_K]}} (v_K - v_M)^2 + \\
\frac{|\mathbf{n}_{[x_M x_\mathrm{e}]}|}{d_{x_M x_\mathrm{e}}} (v_\mathrm{e} - v_M)^2 + \frac{|\mathbf{n}_{[x_M x_L]}|}{d_{[x_M x_L]}} (v_L - v_M)^2 + \frac{|\mathbf{n}_{[x_K x_L]}|}{d_{[x_K x_L]}} (v_L - v_K)^2
\end{bmatrix}.
\end{aligned} \tag{81}$$

From (75) and (81), we choose $C_3 = \frac{1}{\min\left\{\frac{\delta^3}{12}, \frac{\delta}{6}\left(1+\frac{1}{2\delta}\right), \frac{\delta^2}{36}\right\}}$ to satisfy the inequality (72), which is the sum of (81) for all $T \in \mathcal{T}_h^{**}$.

Next, on each $T \in \mathcal{T}_h^{**}$, $P_1\mathbf{v}_h$ is written as

$$P_1\mathbf{v}_h(x) = \begin{cases}
\Pi^0_h\mathbf{v}_h(x) + \nabla P_1\mathbf{v}_h|_T \cdot (x - x_M), & \text{if } x \in P_{x_M}, \\
\Pi^0_h\mathbf{v}_h(x) + \nabla P_1\mathbf{v}_h|_T \cdot (x - x_K), & \text{if } x \in P_{x_K}, \\
\Pi^0_h\mathbf{v}_h(x) + \nabla P_1\mathbf{v}_h|_T \cdot (x - x_L), & \text{if } x \in P_{x_L}, \\
\Pi^0_h\mathbf{v}_h(x) + \nabla P_1\mathbf{v}_h|_T \cdot (x - x_\mathrm{e}), & \text{if } x \in P_{x_\mathrm{e}},
\end{cases} \tag{82}$$

where the restriction $\nabla P_1\mathbf{v}_h|_T$ of $\nabla P_1\mathbf{v}_h$ on T is given as

$$\begin{aligned}
m_T\ \nabla P_1\mathbf{v}_h|_T =& (v_e - v_K)\mathbf{n}_{x_K x_\mathrm{e}} + (v_e - v_L)\mathbf{n}_{x_L x_\mathrm{e}} + (v_e - v_M)\mathbf{n}_{x_M x_\mathrm{e}} \\
&+ (v_L - v_K)\mathbf{n}_{x_K x_L} + (v_K - v_M)\mathbf{n}_{x_M x_K} + (v_L - v_M)\mathbf{n}_{x_M x_L},
\end{aligned} \tag{83}$$

and the operator Π^0_h is defined as given in (51).

The following result is obtained by applying the triangle inequality to (82)

$$\| P_1\mathbf{v}_h \|_{L^2(\Omega)} \leq \| \Pi^0_h\mathbf{v}_h \|_{L^2(\Omega)} + h \| \nabla P_1\mathbf{v}_h \|_{(L^2(\Omega))^2}. \tag{84}$$

By employing the Cauchy–Schwarz inequality in (83), we can continue estimating the terms $\|\nabla P_1 \mathbf{v}_h\|_{(L^2(\Omega))}$ and $\|\Pi_h^0 \mathbf{v}_h\|_{L^2(\Omega)}$ as follows:

$$\begin{aligned}
&\sum_{T\in\mathcal{T}_h^{**}} m_T |\nabla P_1 \mathbf{v}_h| \\
&\leq \sum_{T\in\mathcal{T}_h^{**}} \left[\begin{array}{l} (v_e - v_K)^2 \frac{|\mathbf{n}_{x_K x_\mathrm{e}}|}{d_{x_K x_\mathrm{e}}} + (v_e - v_L)^2 \frac{|\mathbf{n}_{x_L x_\mathrm{e}}|}{d_{x_L x_\mathrm{e}}} + (v_e - v_M)^2 \frac{|\mathbf{n}_{x_M x_\mathrm{e}}|}{d_{x_M x_\mathrm{e}}} \\ +(v_L - v_K)^2 \frac{|\mathbf{n}_{x_K x_L}|}{d_{x_K x_L}} + (v_K - v_M)^2 \frac{|\mathbf{n}_{x_M x_K}|}{d_{x_M x_K}} + (v_L - v_M)^2 \frac{|\mathbf{n}_{x_M x_L}|}{d_{x_M x_L}} \end{array} \right] \\
&\left[\sum_{\substack{T\in\mathcal{T}_h^{**} \\ T=(x_M x_K x_L x_\mathrm{e})}} \sum_{(x_N,x_Q)\in\mathcal{V}_T^{(2)}} |\mathbf{n}_{x_N x_Q}| d_{x_N x_Q} \right].
\end{aligned}$$

Taking note that $m_T = \frac{2}{3} \sum_{(x_N,x_Q)\in\mathcal{V}_T^{(2)}} |\mathbf{n}_{x_N x_Q}| d_{x_N x_Q}$ and using the definition in (52), the above inequality can be rewritten as

$$\|\nabla P_1 \mathbf{v}_h\|^2_{(L^2(\Omega))^3} \leq \frac{3}{2} m_\Omega \, \|\mathbf{v}_h\|^2_{1,\mathcal{T}_h^{**}}, \tag{85}$$

where m_Ω represents the volume of Ω.

According to [17, Lemma 5.3], there exists a positive constant C_4 independent of h such that

$$\|\Pi_h^0 \mathbf{v}_h\|_{L^2(\Omega)} \leq C_4 \|\mathbf{v}_h\|^2_{1,\mathcal{T}_h^{**}}, \quad \forall \mathbf{v}_h \in \mathcal{H}_h. \tag{86}$$

By combining (72) with (84)–(86), one can deduce

$$\|P_1 \mathbf{v}_h\|_{L^2(\Omega)} \leq \left(C_4 + \frac{3}{2} h m_\Omega \right) \|\mathbf{v}_h\|^2_{1,\mathcal{T}_h^{**}} \leq C_3 \left(C_4 + \frac{3}{2} h m_\Omega \right) \|\nabla_\Lambda \mathbf{v}_h\|^2_{(L^2(\Omega))^3}. \tag{87}$$

For a sufficiently small value of h, there exists a positive constant $C_2 > C_3 \left(C_4 + \frac{3}{2} h m_\Omega \right)$ that is independent of h and satisfies the coercive property (69) for the EFC-3DFEMb scheme.

Next, we will prove that the EFC-3DFEMb scheme has the strong consistency property (70).

For any $\varphi \in C_c^\infty(\Omega)$, there exists a vector $\boldsymbol{\varphi}_h$ such that the values of its elements are taken from $(\varphi(x_P))_{x_P\in\mathcal{V}^{**}} \in \mathcal{H}_h^0$. According to [17, Lemma 4.3], there exists a positive constant C_5 that is independent of h, and satisfies

$$\|\nabla_\Lambda \boldsymbol{\varphi}_h - \nabla\varphi\|_{(L^2(\Omega))^3} \leq C_5 h. \tag{88}$$

Combining the result of [18, Lemma 3.1] with this, one can write

$$\|P_1\boldsymbol{\varphi}_h - \varphi\|_{L^2(\Omega)} \leq h\|\nabla\varphi\|_{\left(L^2(\Omega)\right)^3}. \tag{89}$$

After establishing the strong consistency of the EFC-3DFEMb scheme, it is necessary to prove the dual consistency property (71) as follows:

For any $\boldsymbol{\varphi} \in \left(C_c^\infty(\Omega)\right)^3$, the operators I and $\{I_i\}_{i=\overline{1,3}}$ are defined by

$$\begin{aligned}
I(\boldsymbol{\varphi}) &= \int_\Omega \left[\nabla_\Lambda \mathbf{v}_h \cdot \boldsymbol{\varphi} + P_1\mathbf{v}_h \operatorname{div}\boldsymbol{\varphi}\right] dx = I_1(\boldsymbol{\varphi}) + I_2(\boldsymbol{\varphi}) + I_3(\boldsymbol{\varphi}),\\
I_1(\boldsymbol{\varphi}) &= \sum_{T\in\mathcal{T}_{\text{const}}^{**}} m_T \nabla_\Lambda \mathbf{v}_h \cdot \boldsymbol{\varphi}_T\\
&\quad + \sum_{\substack{T\in\mathcal{T}_h^{**}\setminus\{\mathcal{T}_{\text{const}}^{**}\cup\mathcal{T}_\Lambda^{**}\}\\ T:=(x_M x_K x_L x_e)}} \left[m_{T_K}\left(\nabla_\Lambda \mathbf{v}_h\right)_{T_K}\cdot\boldsymbol{\varphi}_{T_K} + m_{T_L}\left(\nabla_\Lambda \mathbf{v}_h\right)_{T_L}\cdot\boldsymbol{\varphi}_{T_L}\right]\\
&\quad + \sum_{T\in\mathcal{T}_\Lambda^{**}} \left[m_{T_K}\left(\nabla_\Lambda \mathbf{v}_h\right)_{T_K}\cdot\boldsymbol{\varphi}_{T_K} + m_{T_L}\left(\nabla_\Lambda \mathbf{v}\right)_{T_L}\cdot\boldsymbol{\varphi}_{T_L}\right],\\
I_2(\boldsymbol{\varphi}) &= \sum_{\substack{T\in\mathcal{T}_h^{**}\\ T:=(x_M x_K x_L x_e)}} \begin{bmatrix} \int_{P_{x_M}} \left(\Pi_h^0\mathbf{v}_h(x)\right)\operatorname{div}\boldsymbol{\varphi}\, dx + \int_{P_{x_K}} \left(\Pi_h^0\mathbf{v}_h(x)\right)\operatorname{div}\boldsymbol{\varphi}\, dx\\ \int_{P_{x_L}} \left(\Pi_h^0\mathbf{v}_h(x)\right)\operatorname{div}\boldsymbol{\varphi}\, dx + \int_{P_{x_e}} \left(\Pi_h^0\mathbf{v}_h(x)\right)\operatorname{div}\boldsymbol{\varphi}\, dx \end{bmatrix},
\end{aligned} \tag{90}$$

$$I_3(\boldsymbol{\varphi}) = \sum_{\substack{T\in\mathcal{T}_h^{**}\\ T:=(x_M x_K x_L x_e)}} \begin{bmatrix} \int_{P_{x_M}} \left(\nabla P_1\mathbf{v}_h|_T \cdot (x - x_M)\right)\operatorname{div}\boldsymbol{\varphi}\, dx\\ + \int_{P_{x_K}} \left(\nabla P_1\mathbf{v}_h|_T \cdot (x - x_K)\right)\operatorname{div}\boldsymbol{\varphi}\, dx\\ \int_{P_{x_L}} \left(\nabla P_1\mathbf{v}_h|_T \cdot (x - x_L)\right)\operatorname{div}\boldsymbol{\varphi}\, dx\\ + \int_{P_{x_e}} \left(\nabla P_1\mathbf{v}_h|_T \cdot (x - x_e)\right)\operatorname{div}\boldsymbol{\varphi}\, dx \end{bmatrix},$$

$$\text{with } \mathbf{v}_h \in \mathcal{H}_h, \quad I_1(\boldsymbol{\varphi}) = \int_\Omega \nabla_\Lambda \mathbf{v}\cdot\boldsymbol{\varphi}\, dx, \quad I_2(\boldsymbol{\varphi}) + I_3(\boldsymbol{\varphi})$$

$$= \sum_{\substack{T\in\mathcal{T}_h^{**}\\ T:=(x_M x_K x_L x_e)}} \int_T \left[P_1\mathbf{v}_h \operatorname{div}\boldsymbol{\varphi}\right] dx.$$

Using the above operators, we can rewrite $\widehat{W}_h(\boldsymbol{\varphi})$ as

$$\widehat{W}_h(\boldsymbol{\varphi}) = \max_{\mathbf{v}_h\in\mathcal{H}_h} \frac{1}{\|\nabla_\Lambda \mathbf{v}_h\|}\int_\Omega \left[\nabla_\Lambda \mathbf{v}_h\cdot\boldsymbol{\varphi} + P_1\mathbf{v}_h \operatorname{div}(\boldsymbol{\varphi})\right] dx = \max_{\mathbf{v}_h\in\mathcal{H}_h} \frac{1}{\|\nabla_\Lambda \mathbf{v}_h\|} I(\boldsymbol{\varphi}).$$

In addition, based on Lemma 1, $I_1(\boldsymbol{\varphi})$ can be rewritten as

$$I_1(\boldsymbol{\varphi}) = \sum_{T\in\mathcal{T}_h^{**}\setminus\mathcal{T}_\Lambda^{**}} \begin{bmatrix} (v_K - v_M)(\mathbf{n}_{x_M x_K} + \boldsymbol{\epsilon}_{x_M x_K}) + (v_L - v_M)(\mathbf{n}_{x_M x_L} + \boldsymbol{\epsilon}_{x_M x_L}) + \\ (v_e - v_M)(\mathbf{n}_{x_M x_e} + \boldsymbol{\epsilon}_{x_M x_e}) + (v_L - v_K)(\mathbf{n}_{x_K x_L} + \boldsymbol{\epsilon}_{x_K x_L}) + \\ (v_e - v_K)(\mathbf{n}_{x_K x_e} + \boldsymbol{\epsilon}_{x_K x_e}) + (v_e - v_L)(\mathbf{n}_{x_L x_e} + \boldsymbol{\epsilon}_{x_L x_e}) \end{bmatrix} \cdot \boldsymbol{\varphi}_T + \sum_{T\in\mathcal{T}_\Lambda^{**}} \left\{ \begin{bmatrix} (v_K - v_M)\boldsymbol{\tau}_{x_M x_K}^{T_K} + (v_L - v_M)\boldsymbol{\tau}_{x_M x_L}^{T_K} + (v_e - v_M)\boldsymbol{\tau}_{x_M x_e}^{T_K} \\ +(v_L - v_K)\boldsymbol{\tau}_{x_K x_L}^{T_K} + (v_e - v_K)\boldsymbol{\tau}_{x_K x_e}^{T_K} + (v_e - v_L)\boldsymbol{\tau}_{x_L x_e}^{T_K} \end{bmatrix} \cdot \boldsymbol{\varphi}_{T_K} + \begin{bmatrix} (v_K - v_M)\boldsymbol{\tau}_{x_M x_K}^{T_L} + (v_L - v_M)\boldsymbol{\tau}_{x_M x_L}^{T_L} + (v_e - v_M)\boldsymbol{\tau}_{x_M x_e}^{T_L} + \\ (v_L - v_K)\boldsymbol{\tau}_{x_K x_L}^{T_L} + (v_e - v_K)\boldsymbol{\tau}_{x_K x_e}^{T_L} + (v_e - v_L)\boldsymbol{\tau}_{x_L x_e}^{T_L} \end{bmatrix} \cdot \boldsymbol{\varphi}_{T_L} \right\}, \tag{91}$$

with $\boldsymbol{\varphi}_T = \frac{1}{m_T}\int_T \boldsymbol{\varphi}\, dx, \boldsymbol{\varphi}_{T_K} = \frac{1}{m_{T_K}}\int_{T_K} \boldsymbol{\varphi}\, dx$ and $\boldsymbol{\varphi}_{T_L} = \frac{1}{m_{T_L}}\int_{T_L} \boldsymbol{\varphi}\, dx$.

By the Green expression, the operator $I_2(\boldsymbol{\varphi})$ can be rewritten as

$$I_2(\boldsymbol{\varphi}) = \sum_{\substack{T\in\mathcal{T}_h^{**} \\ T:=(x_M x_K x_L x_e)}} \begin{bmatrix} (v_M - v_K)\,\boldsymbol{\varphi}_{x_M x_K}\cdot\mathbf{n}_{x_M x_K} + (v_M - v_L)\,\boldsymbol{\varphi}_{x_M x_L}\cdot\mathbf{n}_{x_M x_L} + \\ (v_M - v_e)\,\boldsymbol{\varphi}_{x_M x_e}\cdot\mathbf{n}_{x_M x_e} + (v_K - v_L)\,\boldsymbol{\varphi}_{x_K x_L}\cdot\mathbf{n}_{x_K x_L} + \\ (v_K - v_e)\,\boldsymbol{\varphi}_{x_K x_e}\cdot\mathbf{n}_{x_K x_e} + \left(v_L - v_{C_e}\right)\boldsymbol{\varphi}_{x_L x_e}\cdot\mathbf{n}_{x_L x_e} \end{bmatrix},$$

$$\text{with } \boldsymbol{\varphi}_{x_M x_K} = \frac{1}{|\mathbf{n}_{x_M x_K}|}\int_{\mathbb{f}_{[x_M x_K]}} \boldsymbol{\varphi} d\gamma, \quad \boldsymbol{\varphi}_{x_M x_L} = \frac{1}{|\mathbf{n}_{x_M x_L}|}\int_{\mathbb{f}_{[x_M x_L]}} \boldsymbol{\varphi} d\gamma,$$
$$\boldsymbol{\varphi}_{x_M x_e} = \frac{1}{|\mathbf{n}_{x_M x_e}|}\int_{\mathbb{f}_{[x_M x_e]}} \boldsymbol{\varphi} d\gamma, \quad \boldsymbol{\varphi}_{x_K x_L} = \frac{1}{|\mathbf{n}_{x_K x_L}|}\int_{\mathbb{f}_{[x_K x_L]}} \boldsymbol{\varphi} d\gamma,$$
$$\boldsymbol{\varphi}_{x_K x_e} = \frac{1}{|\mathbf{n}_{x_K x_e}|}\int_{\mathbb{f}_{[x_K x_e]}} \boldsymbol{\varphi} d\gamma, \quad \boldsymbol{\varphi}_{x_L x_e} = \frac{1}{|\mathbf{n}_{x_L x_e}|}\int_{\mathbb{f}_{[x_L x_e]}} \boldsymbol{\varphi} d\gamma. \tag{92}$$

To estimate $I_1(\boldsymbol{\varphi})$ and $I_2(\boldsymbol{\varphi})$, we introduce the operators R_i on the space $\left(C_c^\infty(\Omega)\right)^3$, where i ranges from 1 to 3, as follows:

$$R_1(\boldsymbol{\varphi}) = \sum_{\substack{T\in\mathcal{T}_h^{**}\setminus\mathcal{T}_\Lambda^{**} \\ T:=(x_M x_K x_L x_e)}} \sum_{(x_N,x_Q)\in\mathcal{V}_T^{(2)}} \left(|\mathbf{n}_{x_N x_Q}| + |\boldsymbol{\epsilon}_{x_N x_Q}|\right) d_{x_N x_Q} \left(\boldsymbol{\varphi}_T - \boldsymbol{\varphi}_{x_N x_Q}\right)^2, \tag{93}$$

$$R_2(\boldsymbol{\varphi}) = \sum_{\substack{T\in\mathcal{T}_h^{**}\setminus\mathcal{T}_\Lambda^{**} \\ T:=(x_M x_K x_L x_e)}} (\boldsymbol{\varphi}_T)^2 \sum_{(x_N,x_Q)\in\mathcal{V}_T^{(2)}} \left(\frac{|\boldsymbol{\epsilon}_{x_N x_Q}|}{|\mathbf{n}_{x_N x_Q}|} d_{x_N x_Q}\right), \tag{94}$$

$$R_3(\boldsymbol{\varphi}) = \sum_{\substack{T\in\mathcal{T}_\Lambda^{**} \\ T:=(x_M x_K x_L x_e)}} \sum_{(x_N,x_Q)\in\mathcal{V}_T^{(2)}} \left[|\mathbf{n}_{x_N x_Q}| d_{x_N x_Q} \left(\frac{\boldsymbol{\tau}_{x_N x_Q}^{T_K}\cdot\boldsymbol{\varphi}_{T_K} + \boldsymbol{\tau}_{x_N x_Q}^{T_L}\cdot\boldsymbol{\varphi}_{T_L} - \mathbf{n}_{x_N x_Q}\cdot\boldsymbol{\varphi}_{x_N x_Q}}{|\mathbf{n}_{x_N x_Q}|} \right)^2 \right], \tag{95}$$

for any $\boldsymbol{\varphi} \in \left(C_c^\infty(\Omega)\right)^3$.

Using the above operators R_i for i ranging from 1 to 3, and applying the Cauchy–Schwarz inequality, one obtains

$$|I_1(\boldsymbol{\varphi}) + I_2(\boldsymbol{\varphi})|^2 \leq \|\mathbf{v}\|^2_{1,\mathcal{T}_h^{**}} \left[R_1(\boldsymbol{\varphi}) + R_2(\boldsymbol{\varphi}) + R_3(\boldsymbol{\varphi})\right], \quad \forall \boldsymbol{\varphi} \in \left(C_c^\infty(\Omega)\right)^3. \tag{96}$$

In (93) for $R_1(\boldsymbol{\varphi})$, using the regularity of $\boldsymbol{\varphi} \in \left(C_c^\infty(\Omega)\right)^3$ yields the existence of $C_{\boldsymbol{\varphi}} > 0$, which depends on $\boldsymbol{\varphi}$, such that

$$|\boldsymbol{\varphi}_T - \boldsymbol{\varphi}_{x_N x_Q}|^2 \leq C_{\boldsymbol{\varphi}} h^2, \quad \text{for each } (x_N, x_Q) \in \mathcal{V}_T^{(2)}. \tag{97}$$

Combining the above result with the property (54) in Lemma 1, there exists a positive constant $C_6 > 0$ that is independent of h such that

$$|R_1(\boldsymbol{\varphi})| \leq C_6 m_\Omega h^2 (1 + \boldsymbol{\epsilon}(h)), \quad \text{with } \lim_{h \to 0} \boldsymbol{\epsilon}(h) = 0, \tag{98}$$

where m_Ω represents the volume of the domain Ω.

Hence,

$$|R_1(\boldsymbol{\varphi})| \to 0, \quad \text{as } h \to 0. \tag{99}$$

For $R_2(\boldsymbol{\varphi})$, with property (54), one can obtain

$$|R_2(\boldsymbol{\varphi})| \to 0, \quad \text{as } h \to 0. \tag{100}$$

For $R_3(\boldsymbol{\varphi})$, using the Cauchy–Schwarz inequality, one can find that a positive constant C_7 depends on $\boldsymbol{\varphi}$, such that

$$\begin{aligned}
&\left(\frac{\boldsymbol{\tau}^{T_K}_{x_N x_Q} \cdot \boldsymbol{\varphi}_{T_K} + \boldsymbol{\tau}^{T_L}_{x_N x_Q} \cdot \boldsymbol{\varphi}_{T_L} - \mathbf{n}_{x_N x_Q} \cdot \boldsymbol{\varphi}_{x_N x_Q}}{|\mathbf{n}_{x_N x_Q}|} \right)^2 \\
&= \left[\begin{array}{l} \frac{\boldsymbol{\tau}^{T_K}_{x_N x_Q}}{|\mathbf{n}_{x_N x_Q}|} \cdot \left(\boldsymbol{\varphi}_{T_K} - \boldsymbol{\varphi}_{x_N x_Q}\right) + \frac{\boldsymbol{\tau}^{T_L}_{x_N x_Q}}{|\mathbf{n}_{x_N x_Q}|} \cdot \left(\boldsymbol{\varphi}_{T_L} - \boldsymbol{\varphi}_{x_N x_Q}\right) \\ \quad + \left(\frac{\boldsymbol{\tau}^{T_K}_{x_N x_Q}}{|\mathbf{n}_{x_N x_Q}|} + \frac{\boldsymbol{\tau}^{T_L}_{x_N x_Q}}{|\mathbf{n}_{x_N x_Q}|} - \frac{\mathbf{n}_{x_N x_Q}}{|\mathbf{n}_{x_N x_Q}|} \right) \cdot \boldsymbol{\varphi}_{x_N x_Q} \end{array} \right]^2 \\
&\leq 3 \left[\begin{array}{l} \left(\frac{|\boldsymbol{\tau}^{T_K}_{x_N x_Q}|}{|\mathbf{n}_{x_N x_Q}|} \right)^2 \left(\boldsymbol{\varphi}_{T_K} - \boldsymbol{\varphi}_{x_N x_Q}\right)^2 \\ \quad + \left(\frac{|\boldsymbol{\tau}^{T_L}_{x_N x_Q}|}{|\mathbf{n}_{x_N x_Q}|} \right)^2 \left(\boldsymbol{\varphi}_{T_L} - \boldsymbol{\varphi}_{x_N x_Q}\right)^2 \\ \quad + \left(\frac{|\boldsymbol{\tau}^{T_K}_{x_N x_Q}|}{|\mathbf{n}_{x_N x_Q}|} s + \frac{|\boldsymbol{\tau}^{T_L}_{x_N x_Q}|}{|\mathbf{n}_{x_N x_Q}|} + 1 \right)^2 |\boldsymbol{\varphi}_{x_N x_Q}|^2 \end{array} \right] \leq C_7, \quad \forall (x_N, x_Q) \in \mathcal{V}_T^{(2)}.
\end{aligned} \tag{101}$$

By applying (101) and utilizing $m_T = \frac{2}{3}\sum_{(x_N,x_Q)\in\mathcal{V}_T^{(2)}} d_{x_N x_Q}|\mathbf{n}_{x_N x_Q}|$ in the formula (95), one can find that there exists a positive constant $C_8 > 0$, dependent only on $\boldsymbol{\varphi}$, such that

$$|R_3(\boldsymbol{\varphi})| \leq C_8 \sum_{T\in\mathcal{T}_\Lambda^{**}} m_T. \tag{102}$$

According to [19, Theorem 3.8], it is established that

$$\sum_{T\in\mathcal{T}_\Lambda^{**}} m_T \to 0, \quad \text{as } h \to 0, \tag{103}$$

One can observe that the dimension of the zones where the tensor $\Lambda(x)$ is piecewise Lipschitz continuous is one or two.

From Eqs. (102) and (103), it follows that

$$|R_3(\boldsymbol{\varphi})| \to 0, \quad \text{as } h \to 0. \tag{104}$$

Applying Holder's inequality and utilizing (85) leads to

$$|I_3(\boldsymbol{\varphi})| \leq h \left\|\nabla P_1(\mathbf{v})\right\|_{\left(L^2(\Omega)\right)^3} \left\|\mathrm{div}(\boldsymbol{\varphi})\right\|_{L^2(\Omega)} \leq h\sqrt{\frac{3}{2}m_\Omega}\, \|\mathbf{v}_h\|_{1,\mathcal{T}_h^{**}} \left\|\mathrm{div}(\boldsymbol{\varphi})\right\|_{L^2(\Omega)}, \tag{105}$$

and therefore

$$|I_3(\boldsymbol{\varphi})| \to 0, \quad \text{as } h \to 0. \tag{106}$$

Combining the inequalities (72), (96), (105) and for each $\boldsymbol{\varphi} \in \left(C_c^\infty(\Omega)\right)^3$, one can obtain

$$\begin{aligned}\frac{1}{\left\|\nabla_\Lambda \mathbf{v}_h\right\|_{\left(L^2(\Omega)\right)^3}}|I(\boldsymbol{\varphi})| \leq{}& \frac{\sqrt{C_3}}{\|\mathbf{v}_h\|_{1,\mathcal{T}_h^{**}}}\|\mathbf{v}_h\|_{1,\mathcal{T}_h^{**}}\sqrt{(R_1(\boldsymbol{\varphi}) + R_3(\boldsymbol{\varphi}) + R_2(\boldsymbol{\varphi}))} \\ &+ \frac{\sqrt{C_3}}{\|\mathbf{v}_h\|_{1,\mathcal{T}_h^{**}}} h\sqrt{3m_\Omega}\, \|\mathbf{v}_h\|_{1,\mathcal{T}_h^{**}} \left\|\mathrm{div}(\boldsymbol{\varphi})\right\|_{L^2(\Omega)}, \quad \forall \mathbf{v}_h \in \mathcal{H}_h.\end{aligned} \tag{107}$$

Regarding the convergences of (99), (100), and (104) with the above inequalities, it can be concluded for each $\boldsymbol{\varphi} \in \left(C_c^\infty(\Omega)\right)^3$ that

$$\frac{1}{\left\|\nabla_\Lambda \mathbf{v}_h\right\|_{\left(L^2(\Omega)\right)^3}}|I(\boldsymbol{\varphi})| \to 0, \quad \text{as } h \to 0, \quad \forall \mathbf{v}_h \in \mathcal{H}_h \setminus \{\mathbf{0}\}.$$

As a result, the strong consistency property (71) has been proven. □

Corollary 1 *Let $(\mathcal{H}_h, h, \Phi, \nabla_\Lambda)$ be a family of discretizations in the sense of Definition 1. If the EFC-3DFEMb scheme satisfies the coercive, dual, and strong consistency properties under the assumptions of Proposition 2, then the EFC-3DFEM scheme also satisfies the coercive, dual, and strong consistency properties.*

Proof For any $\mathbf{v}_h \in \mathcal{H}_h$, with the definitions of $\Phi\mathbf{v}_h$ in (26) and $P_1\mathbf{v}_h$ in (48), we get the following inequality:

$$\|\Phi\mathbf{v}_h - P_1\mathbf{v}_h\|_{L^2(\Omega)} \leq h\left(\|\nabla P_1\mathbf{v}_h\|_{(L^2(\Omega))^3} + \|\nabla_\Lambda\mathbf{v}_h\|_{(L^2(\Omega))^3}\right). \tag{108}$$

Substituting (72) and (85) into the above inequality, we get

$$\|\Phi\mathbf{v}_h - P_1\mathbf{v}_h\|_{L^2(\Omega)} \leq C_9 h\|\nabla_\Lambda\mathbf{v}_h\|_{(L^2(\Omega))^3} \tag{109}$$

where C_9 is a positive constant independent of h.

By (109) and the coercivity (69) of P_1, a positive constant C_{10} is defined and independent of h such that

$$\|\Phi\mathbf{v}_h\|_{L^2(\Omega)} \leq \|\Phi\mathbf{v}_h - P_1\mathbf{v}_h\|_{L^2(\Omega)} + \|P_1\mathbf{v}_h\|_{L^2(\Omega)} \leq C_{10}\|\nabla_\Lambda\mathbf{v}_h\|_{(L^2(\Omega))^3}, \tag{110}$$

which means that the EFC-3DFEM scheme is coercive.

Let $\varphi \in C_c^\infty(\Omega)$, and consider a vector $\boldsymbol{\varphi}_h$ whose elements are taken from $(\varphi(x_P))_{x_P\in\mathcal{V}^{**}} \in \mathcal{H}_h$. Utilizing the triangle inequality in (89) and (109), we estimate the error between $\Phi(\boldsymbol{\varphi}_h)$ and φ as follows:

$$\begin{aligned}\|\Phi\boldsymbol{\varphi}_h - \varphi\|_{L^2(\Omega)} &\leq \|\Phi\boldsymbol{\varphi}_h - P_1\boldsymbol{\varphi}_h\|_{L^2(\Omega)} + \|P_1\boldsymbol{\varphi}_h - \varphi\|_{L^2(\Omega)} \\ &\leq h\left[C_9\|\nabla_\Lambda\boldsymbol{\varphi}_h\|_{(L^2(\Omega))^3} + \|\nabla\varphi\|_{(L^2(\Omega))^3}\right].\end{aligned} \tag{111}$$

Hence,

$$\|\Phi\boldsymbol{\varphi}_h - \varphi\|_{L^2(\Omega)} \to 0, \quad \text{as } h \to 0. \tag{112}$$

Combining the above with the convergence of (88), the EFC-3DFEM scheme satisfies the strong consistency property (43). From Proposition 1 and (109), it also satisfies the dual consistency (44). □

5 Numerical experiments

In this section, three benchmark tests [9] are carried out to verify the numerical results for the convergence of EFC-3DFEM scheme with the following methods:

- FEM-T4 – The standard linear finite element method on a tetrahedral mesh [20];
- SUSHI – A scheme using stabilization and hybrid interfaces [21];

- CeVeFE-DDFV – A discrete duality finite volume scheme with cell/vertex/face+edge unknowns [22];
- VAG – The vertex approximate gradient scheme [23]; and
- MFD-GEN – The mimetic finite difference of generalized polyhedral meshes [24];

The above list includes the FEM-T4 method because the EFC-3DFEM method is equivalent to this approach on the tetrahedral subdual mesh $\mathcal{T}_h^{**}$ in the isotropic tensor situation. Except for the FEM-T4 method, the remaining methods satisfy the local conservativity of the fluxes, which is particularly essential for handling heterogeneous, anisotropic (possibly discontinuous) diffusion (e.g., Tests 2 and 3).

The relative errors on the subdual mesh $\mathcal{T}_h^{**}$ in L^2, H^1 semi-norm, and energy norm of proposed EFC-3DFEM scheme denoted by erl2, ergrad, and ener are computed as follows:

$$\text{erl2} = \left(\frac{\sum_{T \in \mathcal{T}_h^{**}} \int_T |u_h - u|^2 dx}{\sum_{T \in \mathcal{T}_h^{**}} \int_T |u|^2 dx} \right)^{1/2}, \tag{113}$$

$$\text{ergrad} = \left(\frac{\sum_{T \in \mathcal{T}_h^{**}} \int_T |\nabla_\Lambda u_h - \nabla u|^2 dx}{\sum_{T \in \mathcal{T}_h^{**}} \int_T \nabla u|^2 dx} \right)^{1/2}, \tag{114}$$

$$\text{ener} = \left(\frac{\sum_{T \in \mathcal{T}_h^{**}} \int_T [\Lambda (\nabla_\Lambda u_h - \nabla u)] \cdot (\nabla_\Lambda u_h - \nabla u) \, dx}{\sum_{T \in \mathcal{T}_h^{**}} \int_T (\Lambda \nabla u) \cdot \nabla u \, dx} \right)^{1/2}, \tag{115}$$

where u is the the exact solution and $\mathbf{u}_h = (u_P)_{x_P \in \mathcal{N}^{**}}$ is the numerical result u_h at vertices of the subdual mesh $\mathcal{T}_h^{**}$. Besides, umin and umax are defined as the minimum and maximum values of the approximate solutions. Additionally, their rates of convergence are expressed for each number of mesh $i \geq 2$ as follows:

$$\text{ratiol2} = -3 \frac{\log (\text{erl2}(i)/\text{erl2}(i-1))}{\log (\text{nu}(i)/\text{nu}(i-1))}, \tag{116}$$

$$\text{ratiograd} = -3 \frac{\log (\text{ergrad}(i)/\text{ergrad}(i-1))}{\log (\text{nu}(i)/\text{nu}(i-1))}, \tag{117}$$

$$\text{ratioener} = -3 \frac{\log (\text{ener}(i)/\text{ener}(i-1))}{\log (\text{nu}(i)/\text{nu}(i-1))}, \tag{118}$$

with nu denotes the number of unknowns in the linear system.

Additionally, four different fundamental mesh types of primal meshes are studied: the uniform tetrahedral mesh (Mesh 1), the checkerboard mesh (Mesh 2), the prism mesh with general bases (Mesh 3), and the locally refined mesh (Mesh 4) (see Fig. 8).

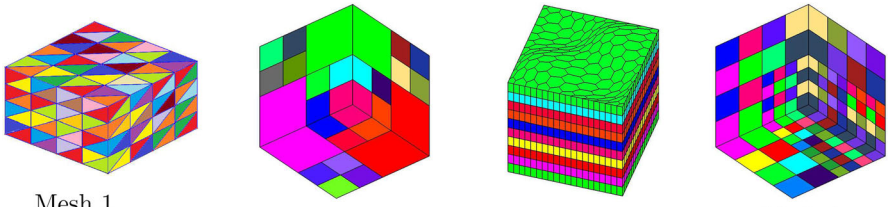

Fig. 8 Four types of primal meshes: (a) Mesh 1: uniform tetrahedral mesh, (b) Mesh 2: checkerboard mesh, (c) Mesh 3: prism mesh with general bases, and (d) Mesh 4: locally refined mesh

Table 1 Convergence of the EFC-3DFEM scheme for Test 1 on Mesh 1

nu	erl	ratioerl	ergrad	ratiograd	ener	ratioener	umin	umax
860	1.133e–02		1.053e–01		1.005e–01		8.555e–03	1.991
6232	3.172e–03	1.929	5.933e–02	0.828	5.667e–02	0.868	2.141e–03	1.998
47,408	8.425e–04	1.960	3.147e–02	0.914	3.007e–02	0.937	5.354e–04	1.999
369,760	2.175e–04	1.977	1.621e–02	0.957	1.548e–02	0.969	1.338e–04	1.999

Test 1 *Mild anisotropy.*

Considering a constant, anisotropic permeability tensor Λ_1 and a regular solution u_1 determined on the unit cubic domain Ω, a non-homogeneous Dirichlet condition on the domain boundary $\partial\Omega$ is as follows:

$$\Lambda_1(x, y, z) = \begin{pmatrix} 1 & 0.5 & 0 \\ 0.5 & 1 & 0.5 \\ 0 & 0.5 & 1 \end{pmatrix}, \tag{119}$$

$$u_1(x, y, z) = 1 + \sin(\pi x) \sin\left(\pi\left(y + \frac{1}{2}\right) \sin\left(\pi\left(z + \frac{1}{3}\right)\right)\right). \tag{120}$$

The minimum and maximum values of the solution u_1 on Ω are equal to 0 and 2, respectively. The primal meshes are Mesh 1 and Mesh 2.

It can be observed in Table 1 that when the mesh is refined, the EFC-3DFEM delivers good convergence and the rate is of 1.9 in L^2-norm, nearly 0.9 in H^1-norm and energy norm. Besides, the EFC-3DFEM scheme is higher accurate than FEM-T4 in the relative errors as indicated in Fig. 9. On a finer mesh of the subdual mesh $\mathcal{T}_h^{**}$, the numerical results are really obtained.

From Table 2, the EFC-3DFEM delivers also good convergence and the rate increases to 1.98 in L^2-norm, 0.947 in H^1-norm and 0.949 in the energy norm. The EFC-3DFEM presents smaller errors in L^2-norm than VAG, CeVeFE-DDFV, and SUSHI schemes as shown Fig. 10 with the same primal mesh size.

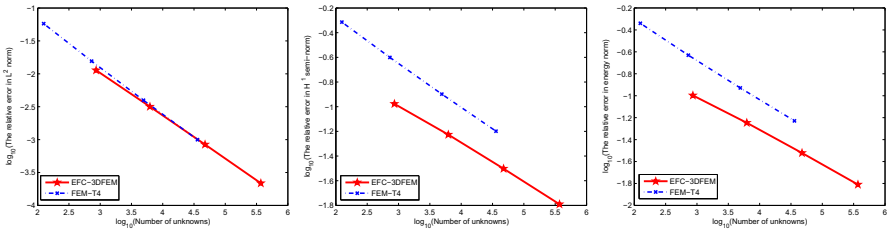

(a) (b) (c)

Fig. 9 The relative errors in L^2 norm (a), H^1 semi-norm (b), and energy norm (c) obtained by using the EFC-3DFEM and FEM-T4 schemes for Test 1 on Mesh 1

Table 2 Convergence of the EFC-3DFEM scheme for Test 1 on Mesh 2

nu	erl	ratioerl	ergrad	ratiograd	ener	ratioener	umin	umax
252	3.348e–02		2.173e–01		2.163e–01		8.555e–03	1.991
1824	1.037e–02	1.776	1.467e–01	0.595	1.448e–01	0.608	2.141e–03	1.997
13,824	2.754e–03	1.964	8.150e–02	0.871	8.03483e–02	0.873	5.354e–04	1.999
107,520	7.098e–04	1.983	4.264e–02	0.947	4.200e–02	0.949	1.338e–04	1.999

Table 3 Convergence results of the EFC-3DFEM scheme for Test 2 on Mesh 3

nu	erl2	ratiol2	ergrad	ratiograd	ener	ratioener	umin	umax
8410	2.923e–02		2.679e–01		2.781e–01		-8.842e–01	1.047
57,420	8.156e–03	1.994	1.074e–01	1.428	1.136e–01	1.398	-8.609e–01	1.049
183,030	3.771e–03	1.996	6.908e–02	1.141	7.405e–02	1.108	-8.641e–01	1.048
421,240	2.175e–03	1.981	5.199e–02	1.023	5.584e–02	1.016	-8.616e–01	1.049

Test 2 *Heterogeneity and anisotropy.*

On the cubic domain Ω of Mesh 3, a second test is considered with smoothly variable permeability tensor as

$$\Lambda_2(x, y, z) = \begin{pmatrix} y^2 + z^2 + 1 & -xy & -xz \\ -zy & x^2 + z^2 + 1 & -yz \\ -xz & -yz & x^2 + y^2 + 1 \end{pmatrix}. \tag{121}$$

A regular solution u_2 is given as

$$u_2(x, y, z) = x^3 y^2 z + x \sin(2\pi xz) \sin(2\pi xy) \sin(2\pi z), \tag{122}$$

which implies a non-homogeneous Dirichlet condition on the boundary $\partial\Omega$. The minimum and maximum values are equal to -0.862 and 1.0487, respectively.

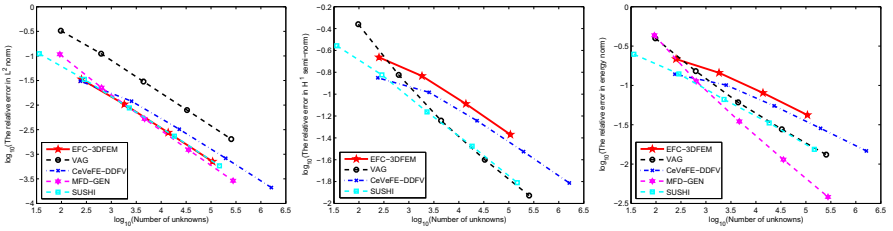

(a) (b) (c)

Fig. 10 The relative errors in L^2 norm (a), H^1 semi-norm (b), and energy norm (c) obtained by using the EFC-3DFEM, VAG, CeVeFE-DDFV, MFD-GEN, and SUSHI schemes for Test 1 on Mesh 2

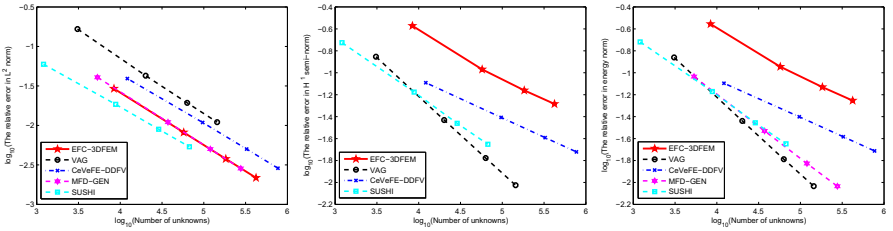

(a) (b) (c)

Fig. 11 The relative errors in L^2 norm (a), H^1 semi-norm (b), and energy norm (c) obtained by using the EFC-3DFEM, VAG, CeVeFE-DDFV, MFD-GEN, and SUSHI schemes for Test 2 on Mesh 3

Test 3 *Strong discontinuous heterogeneous permeability.*

The domain Ω partitioned into the following sub-domains $\overline{\Omega} = \bigcup_{i=1}^{4} \overline{\Omega}_i$ is given by

$$\begin{aligned}
\Omega_1 &= [0, 1] \times [0, 0.5] \times [0, 0.5], \\
\Omega_2 &= [0, 1] \times (0.5, 1] \times [0, 0.5], \\
\Omega_3 &= [0, 1] \times (0.5, 1] \times (0.5, 1], \\
\Omega_4 &= [0, 1] \times [0, 0.5] \times (0.5, 1].
\end{aligned}$$

The permeability tensor is defined as

$$\Lambda_3(x, y, z) = \begin{pmatrix} \alpha_x^i & 0 & 0 \\ 0 & \alpha_y^i & 0 \\ 0 & 0 & \alpha_z^i \end{pmatrix}, \tag{123}$$

and the exact solution is as follows:

$$u_3(x, y, z) = \alpha_i \sin(2\pi x) \sin(2\pi y) \sin(2\pi z), \tag{124}$$

for $(x, y, z) \in \Omega_i$, where the coefficient α_i is given in Table 4. The minimum and maximum values of u_3 on Ω are -100 and 100, respectively.

Table 4 The coefficients $\alpha_x^i, \alpha_y^i, \alpha_z^i, \alpha_i$ for Test 3 on each sub-domain Ω_i

i	1	2	3	4
α_x^i	1	1	1	1
α_y^i	10	0.1	0.01	100
α_z^i	0.01	100	10	0.1
α_i	0.1	10	100	0.01

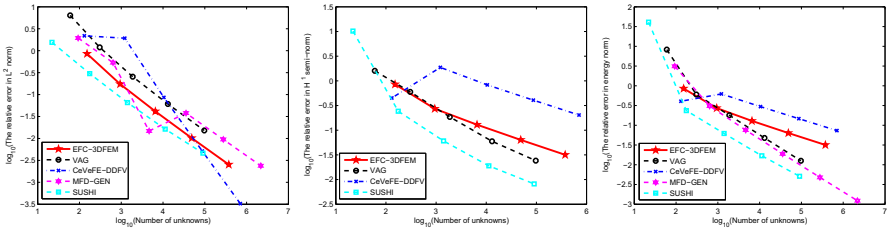

Fig. 12 The relative errors in L^2 norm (a), H^1 semi-norm (b), and energy norm (c) obtained by using the EFC-3DFEM, VAG, CeVeFE-DDFV, MFD-GEN, and SUSHI schemes for Test 3 on Mesh 4

Table 5 Convergence results of the EFC-3DFEM scheme for Test 3 on Mesh 4

nu	erl2	ratiol2	ergrad	ratiograd	ener	ratioener	umin	umax
152	8.505e–01		8.506e–01		8.505e–01		−185.055	185.055
940	1.734e–01	2.618	1.734e–01	1.875	2.723e–01	1.875	−113.946	113.946
6536	4.137e–02	2.217	4.137e–02	1.151	1.291e–01	1.154	−102.948	102.948
48,592	1.020e–02	2.094	1.020e–02	1.060	6.367e–02	1.057	−100.675	100.675
374432	2.542e–03	2.041	2.542e–03	1.024	3.172e–02	1.024	−100.163	100.163

The permeability tensor Λ_3 is discontinuous across the interfaces separating four sub-domains. The exact solution u_3 is designed to be continuous and ensures the conservation of the normal flux across such interfaces. Note that, the homogeneous Dirichlet boundary condition is imposed in this case.

According to Fig. 11 and Table 3 of Test 2 on Mesh 3, Fig. 12 and Table 5 of Test 3 on Mesh 4, the EFC-3DFEM converges and the rates in L^2-norm is nearly 2; however, the H^1-norm and energy norm are nearly 1. Furthermore, with the same mesh size, the EFC-3DFEM offers less L^2-norm error than the VAG, CeVeFE-DDFV, and MFD-GEN schemes on Test 2; and than the VAG, MFD-GEN schemes on Test 3 as shown in Figs. 11 and 12.

Clearly, in the above numerical results, the convergence rate of EFC-3DFEM in L^2-norms, which is nearly 2, is greater than the rate estimated as 1 in (111).

6 Conclusion

The EFC-3DFEM is represented in this research for three-dimensional heterogeneous and anisotropic diffusion problems on generic meshes with discontinuities in the permeability tensor Λ. A primal mesh, a dual mesh, and a tetrahedral subdual mesh were used in the design. Based on the results in this study, the following conclusions can be drawn:

- The EFC-3DFEM possesses four important properties: (i) The stiffness matrix is symmetric and positive definite, (ii) The discrete unknowns are linear combinations at the center points and edge points of the primal mesh, (iii) It benefits from the local continuity of numerical fluxes, and (iv) Leveraging the ability to construct the dual mesh in complex geometric domains (see Remark 1), the subdual mesh is also constructed to align with real-world geometry.
- Within a rigorous theoretical framework, we demonstrate the convergence of the approximate solution for the full diffusion tensor (possibly discontinuous) and general polyhedral meshes.
- The construction of the dual and subdual meshes (see Remark 7) constitutes the core aspect of the macroelement technique [8]. This construction ensures stability by employing this technique when extended to address the three-dimensional Stokes, Oseen, Navier Stokes problems, including cases with variable viscosity, as demonstrated in the two-dimensional case [25].
- The numerical results indicate that the convergence rates are nearly 2 in the L^2-norm. In the cases of the H^1-norm and energy norm, the rates are close to 1, as expected.
- Furthermore, the method is facilitated for direct implementation in the conventional finite element codes based on tetrahedral meshes.

Acknowledgements This research is funded by Vietnam National Foundation for Science and Technology Development (NAFOSTED) under grant number 107.02 – 2021.75.

References

1. Lai X, Sheng Z, Yuan G (2015) A finite volume scheme for three-dimensional diffusion equations. Commun Comput Phys 18(3):650–672
2. Droniou J, Eymard R (2006) A mixed finite volume scheme for anisotropic diffusion problems on any grid. Numer Math 105:35–71
3. Eymard R, Herbin R, Guichard C, Masson R (2012) Vertex-centred discretization of multiphase compositional Darcy flows on general meshes. Comput Geosci 16(4):987–1005
4. Coudière Y, Hubert F (2011) A 3D discrete duality finite volume method for nonlinear elliptic equations. SIAM J Sci Comput 33(4):1739–1764
5. Andreianov B, Hubert F, Krell S (2011) Benchmark 3D: a version of the DDFV scheme with Cell/Vertex unknowns on general meshes. In: Fořt J, Fürst J, Halama J, Herbin R, Hubert F (eds) Finite volumes for complex applications VI—problems & perspectives. Springer, Berlin, pp 937–948
6. Coudiére Y, Pierre C (2011) Benchmark 3D: CeVe-DDFV, a discrete duality scheme with Cell/Vertex unknowns. In: Fořt J, Fürst J, Halama J, Herbin R, Hubert F (eds) Finite volumes for complex applications VI—problems & perspectives, pp 1043–1053. Springer, Berlin
7. Coudière Y, Pierre C, Rousseau O (2009) A 2D/3D discrete duality finite volume scheme. Application to ECG simulation. IJFV Int J Finite Vol 6(1):1–24

8. Stenberg R (1988) Error analysis of some finite element methods for the Stokes problems. In: INRIA Research Report, vol 948
9. Eymard R, Henry G, Herbin R, Hubert F, Klöfkorn R, Manzini G (2011) 3D benchmark on discretization schemes for anisotropic diffusion problems on general grids. In: Fořt J, Fürst J, Halama J, Herbin R, Hubert F (eds) Finite volumes for complex applications VI—problems & perspectives, pp 895–930. Springer, Berlin
10. Garimella RV, Kim J, Berndt M (2014) Polyhedral mesh generation and optimization for non-manifold domains. In: Sarrate J, Staten M (eds) Proceedings of the 22nd International Meshing Roundtable, pp 313–330. Springer, Cham
11. Phuong Hoang TT, Hai Vo DC, Hai Ong T (2017) A low-order finite element method for three dimensional linear elasticity problems with general meshes. Comput Math Appl 74:1379–1398
12. Garimella RV, Kim J, Berndt M (2014) Polyhedral mesh generation and optimization for non-manifold domains. In: Proceedings of the 22nd International Meshing Roundtable, pp 313–330. Springer, Cham
13. Lee SY (2015) Polyhedral mesh generation and a treatise on concave geometrical edges. Procedia Eng 124:174–186
14. Sang Yong Lee (2015) Polyhedral mesh generation and a treatise on concave geometrical edges. Procedia Eng 124:174–186
15. Zhang F (2005) The Schur complement and its applications. Springer, New York
16. Eymard R, Guichard C, Herbin R (2012) Small-stencil 3D schemes for diffusive flows in porous media. ESAIM: M2AN 46:265–290
17. Eymard R, Gallouët T, Herbin R (2010) Discretization of heterogeneous and anisotropic diffusion problems on general non-conforming meshes. Sushi: a scheme using stabilization and hybrid interfaces. IMA J Numer Anal 30(4):1009–1034
18. Eymard R, Herbin R, Rhoudaf M (2011) Approximation of the biharmonic problem using P_1 finite elements. J Numer Math 19(1):1–26
19. Drouniou J, Le Potier C (2011) Construction and convergence study of scheme preserving the elliptic local maximum principle. SIAM J Numer Anal 48:459–490
20. Amor H, Bourgeois M, Mathieu G (2011) Benchmark 3D: a linear finite element solver. In: Fořt J, Fürst J, Halama J, Herbin R, Hubert F (eds) Finite volumes for complex applications VI—problems & perspectives, pp 931–935. Springer, Berlin
21. Eymard R, Gallouët T, Herbin R (2011) Benchmark 3D: the SUSHI scheme. In: Fořt J, Fürst J, Halama J, Herbin R, Hubert F (eds) Finite volumes for complex applications VI—problems & perspectives, pp 1005–1012. Springer, Berlin
22. Coudiére Y, Hubert F, Manzini G (2011) Benchmark 3D: CeVeFE-DDFV, a discrete duality scheme with cell/vertex/face+edge unknowns. In: Fořt J, Fürst J, Halama J, Herbin R, Hubert F (eds) Finite volumes for complex applications VI—problems & perspectives, pp 977–984. Springer, Berlin
23. Eymard R, Guichard C, Herbin R (2011) Benchmark 3D: the VAG scheme. In: Fořt J, Fürst J, Halama J, Herbin R, Hubert F (eds) Finite volumes for complex applications VI—problems & perspectives, pp 1013–1022. Springer, Berlin
24. Lipnikov K, Manzini G (2011) Benchmark 3D: Mimetic finite difference method for generalized polyhedral meshes. In: Fořt J, Fürst J, Halama J, Herbin R, Hubert F (eds) Finite volumes for complex applications VI—problems & perspectives, pp 1035–1042. Springer, Berlin
25. Du Nguyen H, Ong TH (2023) A staggered cell-centered finite element method for Stokes problems with variable viscosity on general meshes. Numer Methods Partial Differ Equ 39(2):1729–1766